AUTONOMOUS SHUTTLING DRIVEN BY AN OSCILLATING REACTION: PROOF OF PRINCIPLE IN A CUCURBIT[7]URIL BODIPY PSEUDOROTAXANE

A THESIS

SUBMITTED TO THE DEPARTMENT OF CHEMISTRY

AND THE GRADUATE SCHOOL OF ENGINEERING AND SCIENCE

OF BİLKENT UNIVERSITY

IN PARTIAL FULFILLMENT OF THE REQUIREMENTS

FOR THE DEGREE OF

MASTER OF SCIENCE

By

FATMA TUBA YAŞAR

February, 2013

I certify that I have read this thesis and that in my opinion it is fully adequate, in scope and in quality, as a thesis for the degree of Master of Science.

…….

Prof. Dr. Engin U. Akkaya (Advisor)

I certify that I have read this thesis and that in my opinion it is fully adequate, in scope and in quality, as a thesis for the degree of Master of Science.

…….

Assist. Prof. Dr. Özgür Altan Bozdemir

I certify that I have read this thesis and that in my opinion it is fully adequate, in scope and in quality, as a thesis for the degree of Master of Science.

…….

Assist. Prof. Dr. Serdar Atılgan

Approved for the Graduate School of Engineering and Science:

…….

Prof. Dr. Levent Onural

Director of the Graduate School

ABSTRACT

AUTONOMOUS SHUTTLING DRIVEN BY AN OSCILLATING REACTION: PROOF OF PRINCIPLE IN A CUCURBIT[7]URIL-BODIPY PSEUDOROTAXANE

Fatma Tuba Yaşar
M.S. in Department of Chemistry
Supervisor: Prof. Dr. Engin U. Akkaya
February, 2013

Miniaturization is a fundamental part of modern technology. Therefore, designing macroscopic machines at molecular level becomes important in terms of mimicking the nature. Despite the numerous molecular machines that were reported in the literature, coupling this design with oscillating reactions to achieve autonomous shuttling was not tried previously. In this thesis, we proposed a novel design for this purpose. Initiating molecular shuttling by oscillating reactions and controlling this shuttling were successfully achieved through a rational design.

Oscillating reactions intrigued chemists for a long time, in this work; we propose to utilize oscillations in pH to move the two components of a pseudorotaxane in relation to each other. In a well behaved oscillatory system, the shuttling could be sustained as long as the oscillations continue. This is the first demonstration of a molecular shuttle system in which the "mobile" component is moving from one station to another in an autonomous fashion. This kind of chemical coupling of an energetically favorable reaction to molecular motion is reminiscent of many biological analogs and therefore highly exciting. Bipyridinium dication substituted BODIPY fluorophore, with a terminal carboxylic acid provides two alternative stations for cucurbit[7]uril (CB7). Changing pH from basic to acidic media results a shuttling of CB7 from one station to another. In addition, the shuttling is accompanied by a change in the emissive properties of the BODIPY dye, which is only observed in the presence of CB7. More striking, it is a demonstration of autonomous shuttling of the pseudorotoxane system in an oscillating pH system.

Keywords: Boradiazaindacene (Bodipy), psedorotaxane, oscillating reactions, cucurbit[7]uril

ÖZET

OSİLASYON REAKSİYONLARI İLE KONTROL EDİLEN OTONOM YERDEĞİŞTİRME: KÜKÜRBİT[7]ÜRİL-BODIPY PSÖDOROTAKSANI KULLANARAK İLKESEL DOĞRULAMA

Fatma Tuba Yaşar
Kimya, Yüksek Lisans
Tez Yöneticisi: Prof. Dr. Engin U. Akkaya
Şubat, 2013

Minyatürleştirme modern teknolojinin temel bir parçasıdır. Bu yüzden makroskopik makineleri moleküler düzeyde tasarlamak doğayı taklit etmek açısından önemlidir. Literatürde yayınlanan çok sayıda moleküler makinenin varlığına rağmen, bu dizaynı otonom yer değiştirmeyi gerçekleştirmesi için osilasyon reaksiyonları ile birleştirmek günümüzde halen yüksek öneme sahiptir. Bu amaca yönelik olarak da, bu çalışmada umut vadeden yöntemler geliştirilmiştir. Moleküler yer değiştirmeyi osilasyon reaksiyonları ile başlatmak ve bu hareketi kontrol etmek rasyonel bir tasarım ile başarılı bir şekilde gerçekleştirilmiştir.

Osilasyon reaksiyonları uzun zamandır kimyacıların ilgisini çekmiştir. Bu çalışmada pH değişimindeki osilasyonlardan yararlanarak psödorotaksanın iki elemanının birbirlerine bağlı olarak hareket etmesi tasarlanmıştır. Bilindiği gibi, düzgün salınımlı osilasyon sistemlerinde yer değiştirme osilasyonlar sürdükçe devam eder. Bu çalışma, 'hareketli' bileşenin bir istasyondan diğerine otonom olarak yer değiştirdiği ilk moleküler mekik sistemi göstergesidir. Bu tarz enerjik olarak tercih edilen reaksiyonun, moleküler hareket ile kimyasal birleşimi birçok biyolojik analoğu hatırlatır ve dolayısıyla yüksek öneme sahiptir. Bipiridin dikatyonu ve uç kısımdaki karboksilik asit ile fonksiyonlandırılmış olan BODIPY boyası, kükürbit[7]üril (CB7) için alternatif iki istasyon sağlar. pH'ın bazik ortamdan asidik ortama geçirilmesi CB7'nin bir istasyondan diğerine yer değiştirmesini sağlamaktadır. Bu yer değiştirme, CB7'nin varlığında BODIPY boyasının emisyon özelliğindeki değişim ile de gözlemlenmiştir. Sonuç olarak, salınım yapan pH sistemi içerisinde, psödorotaksanın otonom yer değiştirmesi sağlanmıştır.

Anahtar Kelimeler: Bodipy, psödorotaksan, osilasyon reaksiyonları, kükürbit[7]üril

Dedicated to my mother and sister

ACKNOWLEDGEMENTS

First and foremost I would like to express my sincere appreciation to my research supervisor Prof. Engin Umut Akkaya. I would like to thank him for taking me as his student and for everything he has done for me in these last four years. It would have been impossible for me to accomplish the work without his kindest guidance, support, encouragement, and patience as well as happiness. I consider it a great privilege to have been his student, and I would like to take this opportunity to offer my deepest gratitude for everything he has done for me. It has been a pleasure studying in his research group.

I would like to extend special thanks to Onur Büyükçakır and Ruslan Guliyev for their advice on my research and the precious time they have shared with me through my master studies. Other than being an outstanding collaborator, they are great lab partners and also good friends.

I also would like to express my appreciation to all of those with whom I have had the pleasure to work within the past four years. I am sincerely grateful to my colleagues Yusuf Çakmak and his good wife Sündüs Erbaş Çakmak, Tuğba Özdemir Kütük, Safacan Kölemen and Bilal Kılıç for support and understanding during the course of this research project. It has been a pleasure working with group members of Akkaya Lab, both past and present, including Dr. Özgür Altan Bozdemir, Dr. Fazlı Sözmen, Dr. Murat Işık, Dr. Cihan Gündüz, Muhammed Büyüktemiz, Ahmet Atılgan, Bilal Uyar, Ziya Köstereli, Şeyma Öztürk, Nisa Yeşilgül, Tuğrul Nalbantoğlu, Gülcihan Gülseren, Merve Kaplan, Hande Boyacı-Selçuk, Sencer Selçuk, Fatma Pir Çakmak, İlke Turan Şimşek, Hatice Turgut, Özge Yılmaz, Gizem Çeltek, Dr. Seda Demirel, Dr. Esra Eçik Tanrıverdi and others. I thank them all for helpful discussions and collaborations as well as for their friendship.

I would like to thank my close friends, Tuğçe Durgut and Yiğit Altay, I have met them here at Bilkent University, who have made my time meaningful during my studies. I would like to thank both of them for all the fun we have had in the last seven years.

I have received great support, encouragement and companionship from Özlem Ünal, Gözde Barım, Menekşe Koca and Seda Selçuk in both my personal life and academic study during the past few years. I thank them all from the bottom of my heart for their valuable friendship.

Last but not the least, I would like to thank my mother, Fevziye Sert, and my sister, Zeynep Tuçe Yaşar. Nobody has been more important to me in the world than my family. There is no word to express my gratitude to my family for their love, support and encouragement during my study in Ankara. Their unconditional love, continuous support and understanding for what I am doing and what I want to do brings me there. I owe them a lot for supporting me spiritually and genuinely throughout my life.

CONTENTS

CHAPTERS

LIST OF FIGURES

LIST OF ABBREVIATIONS

CB[n]	Cucurbit[n]uril,where n=5,6,7,8,10
Bpy	4,4'-bipyridine
BODIPY	Boradiazaindacene
TLC	Thin layer chromatography
NMR	Nuclear magnetic resonance
UV-VIS	Ultraviole Visible
MeCN	Acetonitrile
PET	Photoinduced Electron Transfer
PCT	Photoinduced Charge Transfer
CSTR	Continuous-flow stirred tank reactor
HOMO	Highest Occupied Molecular Orbital
LUMO	Lowest Unoccupied Molecular Orbital
MALDI	Matrix-Assisted Laser Desorption/Ionization
FL	Fluorophore
TOF	Time of Flight
Et_3N	Triethylamine
MS	Mass Spectroscopy
$CHCl_3$	Chloroform
CH_2Cl_2	Dichloromethane
MeOH	Methanol

CHAPTER 1

1. INTRODUCTION

Construction of original molecular devices and machines has an important role in the progress of human civilization. These devices can be very big or small depending on their usage in different areas. In this case, miniaturization which is a heart of modern technology plays a crucial role in the design of these devices.

Supramolecular chemistry spreads out after C.J. Pederson[1], D.J. Cram[2], and J. -M. Lehn[3] took the Nobel Prize in Chemistry in 1937. Depending on the supramolecular studies, it is observed that molecules are much more convenient building blocks than atoms in the design of molecular machines and nanoscale devices. This idea arises from many reasons. First of all, molecules are very stable species whereas atoms are not. This provides scientists to handle easier with molecules compared to atoms. Secondly, in order to construct molecular machines and nanoscale devices, nature starts from molecules, not from atoms. Third of all, most experiments are carried out with molecules in the laboratories. Finally, molecules have device related properties. These properties can be controlled by photochemical and electrochemical inputs. At the end, having these advantages offers new approaches in the design of self-assembled structures for the molecules.

Device and machines are composed of different components to accomplish a specific function in the macroscopic world. Each component performs a simple action whereas complex device performs more complicated and difficult task. For example, the function from hairdryer can be taken by the iterative operations of a switch, a heater, and a fan which is indicated in Figure 1. Therefore, macroscopic concepts of a device and a machine can be extended to the molecular level.[4] A *molecular device* can be classified as an assembly of a distinct number of molecular components which have a capability to accomplish certain function. Each molecular component has single action whereas the complete assembly has more complex function that results from the cooperation of a variety of components. A *molecular machine* is a specific

type of molecular device which display changes as a result of external stimulus.[5] At the end, components show alterations in their positions.

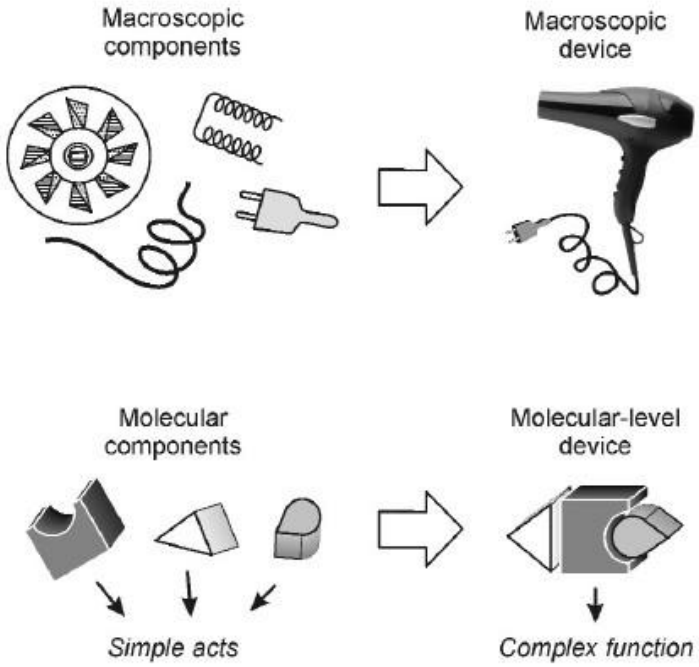

Figure 1. Extension of the macroscopic device concept to the molecular level.[6]

Although nature provides a great number of molecular machines and motors that have high structural complexity, chemists are concerned about developing of simpler artificial systems. Rotaxanes and pseudorotaxanes are the possible candidate molecules from interlocked chemical compounds in the construction of molecular machines. Development of molecular machines requires challenging design, synthesis and investigation. This effort is not only the aim of basic research, but also for the improvement of nanoscience and successive progress of nanotechnology.

All in all, the idea of constructing molecular level machines and devices arises from the great progress of molecular biology. Molecular biologists try to reveal the logic of natural machines that compose the material base of life. Although bottom-up construction of machines and devices similar to nature is difficult, chemists have tried to construct much simpler artificial systems. In this way, it is not necessary to mimic the complexity of biological structures. If the synthetic talent is combined with device-driven properties by chemists, it can lead to outstanding achievements in this field.

CHAPTER 2

2. BACKGROUND

2.1. Concepts in Supramolecular Chemistry

Supramolecular chemistry can be defined as 'chemistry beyond the molecules'. In the design of molecular devices, some functional components are necessary. These photoactive, electroactive and ionactive functional components lead to promising achievements in molecular recognition. In recent years, various receptors for specific substrates were published for the use of molecular recognition. The proper functionalized receptors can be used in supramolecular catalysis and selective transport processes. For all of these processes molecular information is necessary and this should be kept in the components to perform mission in molecular interactions.

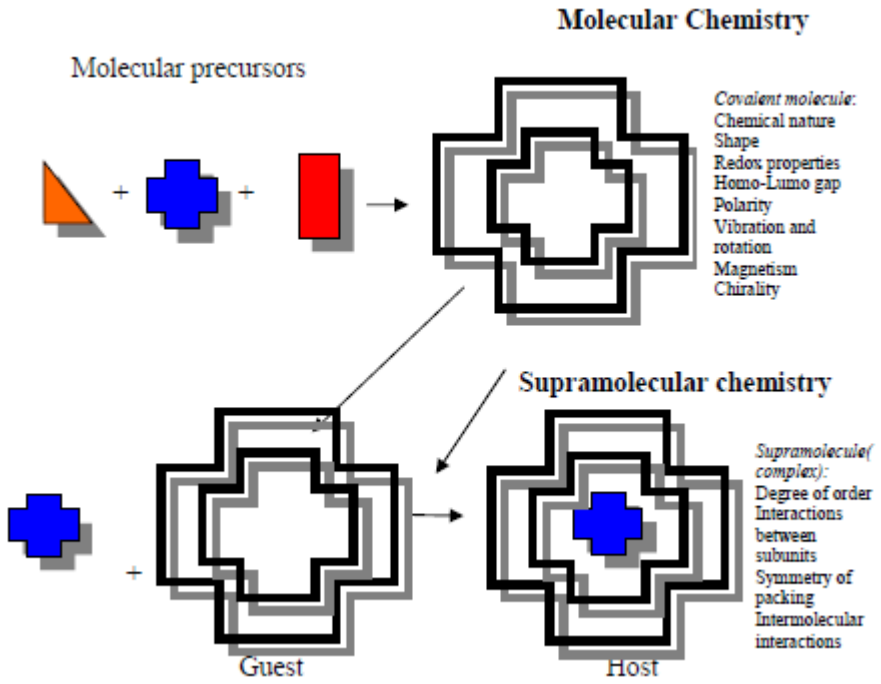

Figure 2. Comparison between the scope of molecular and supramolecular chemistry according to Lehn.[7]

2.1.1. Host-Guest Chemistry

Host-guest chemistry is an important class of supramolecular chemistry and defined as a combination of two or more molecules or ions to form a complex in unique structural relationship by intermolecular forces such as hydrogen bonding and ion-ion interactions.[7] A host-guest complex contains two molecules that are host molecule and guest molecule. The host molecule is generally an organic molecule or ion and has convergent binding sites whereas the guest molecule is defined as a molecule that has divergent binding sites such as antigens. Host-guest chemistry can be used during the study of inclusion complexes, clathrates, cavitates and molecular tweezers. It is an important concept in diverse application areas, such as molecular switches and machines, molecular recognition, catalysis, molecular complexation, drug delivery and extraction and separation of mixtures.

2.1.2. Molecular Recognition

In molecular recognition, non-covalent interactions are used to achieve a binding of host molecule to the guest molecule. Hydrogen bonding and electrostatic interactions are classified as weak intermolecular interactions which plays a crucial role in this process. Normally, they have an effect on short distance. The two molecules fit together in an optimal manner as long as they have the capability to recognize each other.

2.2. Molecular Machines

Interlocked molecules which have multiple metastable states attract considerably an important attention due to the potential applications in molecular device manufacturing.[8] Switching between these metastable states can be achieved via acid-base chemistry[9], electrochemical[10] and photochemical[11] means. These switchable systems are classified as molecular machines[12] and they showed a great progress and increasing elegance in their design in recent years. The basic construction of molecular machines is very simple. They contain a rigid ‘axle’ component and a mobile ‘wheel’ component. The wheel component can positioned at two or more different locations along the axle through the non-covalent interactions such as metal coordination, π-π interaction, hydrogen bonding,

electrostatic interactions (ion-ion, ion-dipole, and dipole-dipole) and hydrophilic and hydrophobic interactions.

When axle is forced to locate inside the macrocycle within stopper groups, it is called rotaxane. The word of ‘rotaxane’ is derived from a Latin and ‘rota’ represents for ‘wheel’ component whereas ‘axis’ stands for ‘axle’ component. In contrast, non-covalent interactions play an important role to hold the macrocycle onto the axle in the pseudorotaxanes. Since there are no stopper groups located in the axle component in the pseudorotaxane.

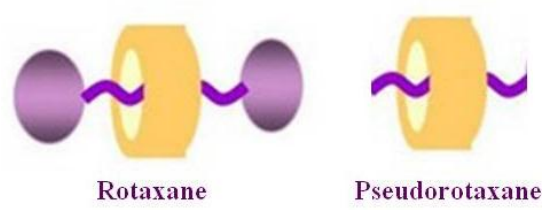

Figure 3. Schematic representation of a rotaxane and a pseudorotaxane.

2.3. Molecular Machines Based On Rotaxanes and Pseudorotaxanes

When molecular machine moves from one station to another with doing mechanical work is an important issue in modern technology. Since linear like reversible movements are essential components of nature. In the artificial macroscopic world, machines are powered by engines which have linear movements. By the synthetic discovery of rotaxanes and pseudorotaxanes, this idea can be used in artificial molecular level. Although these artificial systems have some synthetic challenge, they are different in terms of working pirinciple. They can be powered by chemical, photochemical or electrochemical inputs.[13]

2.3.1. An Acid-Base Controlled Molecular Shuttle

In rotaxanes, it is possible to switch the wheel component from one recognition site to another by external stimulus. A system which is controlled by chemically is shown in Figure 4.[14] This chemically controllable system contains dibenzo[24]crown-8 as a macrocycle and dialkylammonium center and 4,4’-bipyridinium unit as stations. Anthracene moiety was used as stopper group and its absorption and luminescence

properties were used in order to examine the state of the system. As it is stated before, the position of the rotaxane depends on the non-covalent interactions. Hydrogen bonding interactions between the macrocycle and the ammonium center is dominant compared to the ion-dipole interactions of macrocycle with the bipyridinium unit. Therefore, there is two possible locations that macrocycle exists depending on the pH of the media. Under basic conditions, deprotonation of the ammonium center exists and this leads to a displacement of macrocycle from to the bipyridinium unit. However, under acidic conditions, ammonium center was protonated and the macrocycle moves back to its original state. This switching process can be investigated by ^{1}H-NMR spectroscopy and also by electrochemical and photophysical measurements. At the end, it was concluded that as they supply acid and base to the system, the mechanical movement continues as a reversible fashion.

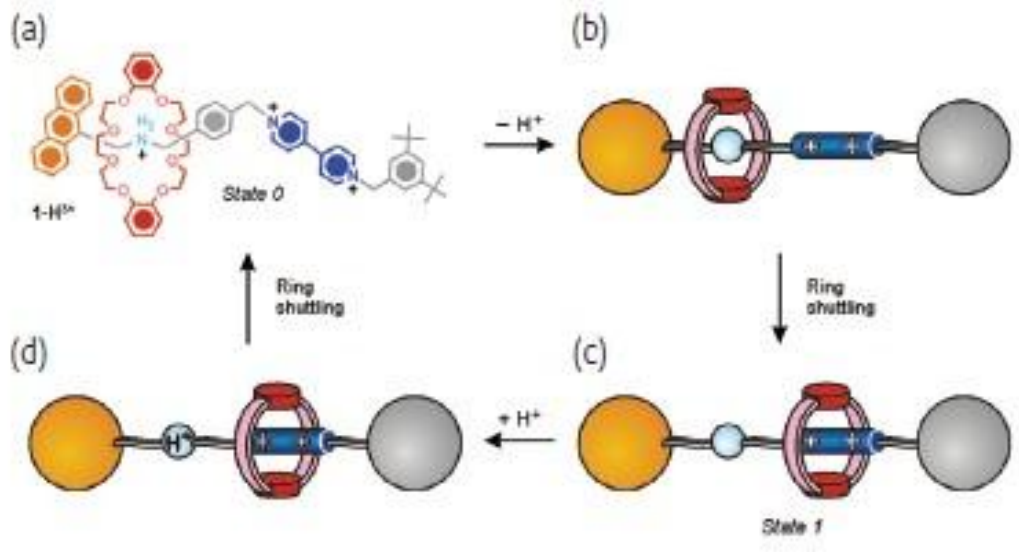

Figure 4. A chemically controllable molecular shuttle controlled by acid-base chemical stimulation in CH_3CN solution.[14]

Later on, this idea was extended to a trifurcated system which contains two stations and each of it has three arms.[15] In each tripod components contain one ammonium center and one 4,4'-bipyridinium unit. Each three compartment are interlocked by the tritopic host and this host molecule serves as a platform which can be made to end at two different levels. In order to prevent the loss of the platform, three legs of the tripod have bulky feet groups. As shown in Figure 5 (state 0), the tritopic host is

located at the ‘upper’ level and ammonium centers were surrounded by three rings. Since strong hydrogen bonding interactions become dominant against the π-π stacking forces between the aromatic units of the platform and tripod components. Addition of base results a deprotonation of the ammonium center and therefore the platform moves to the ‘lower’ level and in this case the bipyridinium units were surrounded by three crown ether rings. Addition of subsequent acid results protonation of ammonium centers and platform moves back to its original state, ‘upper’ level. This ‘up and down’ approach was a mimic of elevator like motion and this system was a demonstration of artificial molecular elevator. This movement can be observed many times as a proof of quantitative switching. ^{1}H NMR spectroscopy, electrochemistry, and absorption and fluorescence spectroscopy were used in order to observe the ‘up and down’ movement.

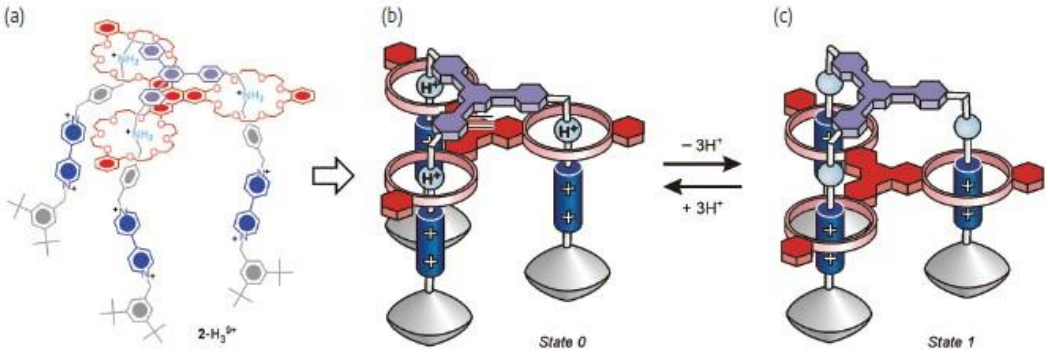

Figure 5. An acid/base controllable molecular elevator.[15]

It should be kept in mind that chemically controlled mechanical motion can be used for the development of drug delivery systems. Since the uptake and release of guest molecule can be controlled by additions of acid and base. Position of the bipyridinium legs can lead different modifications such as closing and opening of a large cavity.

2.3.2. A Light-Driven Molecular Shuttle

Light is the most important component in the design of artificial molecular machines. In order to demonstrate the photoinduced shuttling, the following molecule which is indicated in Figure 6 was synthesized.[16] This rotaxane was composed of six components. In this design, R represents the donor-acceptor macrocycle; P stands for

the stopper and 4, 4'-bipyridinium unit and 3, 3'-dimethyl-4, 4'-bipyridinium unit are the electron accepting stations. *p*-terphenyl-type ring system was used as a rigid spacer (S) whereas tetraarylmethane group was used as a second stopper (T). The rotaxane was characterized by both ^{1}H NMR spectroscopy and mass spectroscopy. At first R component is located on the A_1 unit since this station is better electron-acceptor unit compared to the other one. In order to deduce the information about the photoinduced abacus-like molecular movement between the stations A_1 and A_2, two strategies were developed. These are called as intra-molecular mechanism and sacrificial mechanism, respectively. In the intra-molecular mechanism, only rotaxane components were involved in the process and in the sacrificial mechanism, external reactants were necessary.

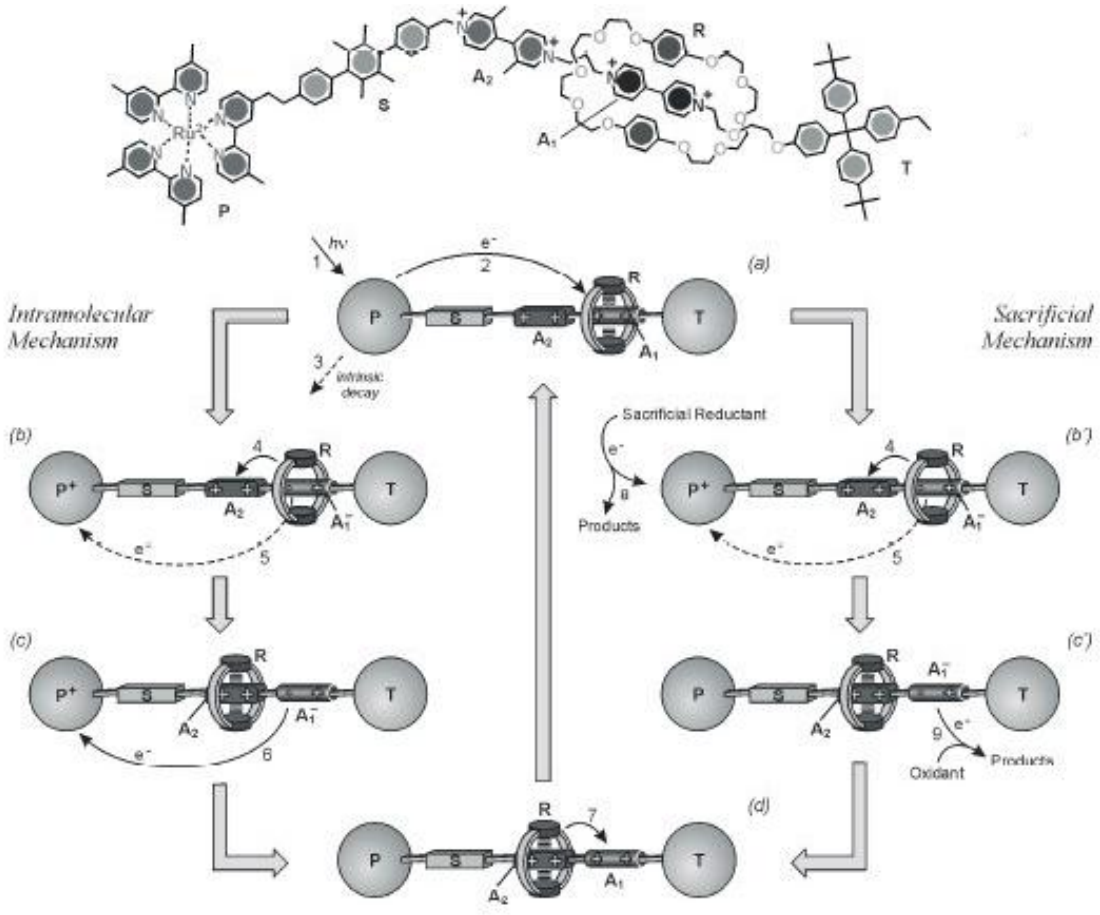

Figure 6. Structural formula of the rotaxane and schematic representation of the intramolecular (left) and sacrificial (right) mechanisms for the photoinduced shuttling movement of macrocycle R between the two stations A_1 and A_2.

The intramolecular mechanism which was represented in the left part of the Figure 6 involves 4 operations.

(a) Destabilization of the stable translational isomer: photoactive unit was excited with light then electron transfer of an electron from excited state to the A_1 station occurs.

(b) Ring displacement: the ring goes from station A_1 to A_2.

(c) Electronic rest: a back electron-transfer from the reduced station A_1 to the oxidized unit P occurs.

(d) Nuclear reset: as a consequence of the electronic reset, back movement of the ring from A_2 to A_1 takes place.

The sacrificial mechanism was used less and it was illustrated in the right part of the Figure 6:

(a) Destabilization of the stable translational isomer: previous mechanism is valid as in the intra-molecular mechanism.

(b') Ring displacement after scavenging of the oxidized photoactive unit: displacement of the ring R to A_2 takes place.

(c) Electronic reset: restration of the electron-acceptor power of the A_1 station is obtained.

(d) Nuclear reset: previous mechanism is valid as in the intra-molecular mechanism.

According to the results, it is observed that sacrificial mechanism is more successful than the intra-molecular mechanism. Sacrificial mechanism is rather rare compared to the intra-molecular mechanism, since it causes the formation of waste products.

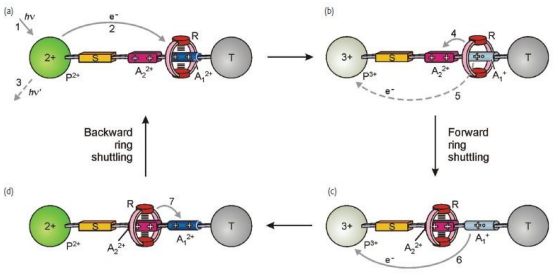

Figure 7. Operation scheme of rotaxane as an autonomous 'four stroke' molecular shuttle powered by light.[17]

2.4. Cucurbit[n]urils

Cucurbiturils are an interesting class of molecules with excellent host properties.[18] The cucurbit[n]urils (where n is commonly 5-8 and 10) are a branch of host molecules which contain paired-methylene bridged glycouril units. They have carbonyl linked portals which provides hydrophobic cavity of low polarizability. The name of the 'cucurbituril' comes from the similarity of the shape of pumpkin family of *Cucurbitaceae*.[19] They have highly selective affinities to different host molecules such as viologens, napthols, etc because of their size-tunable properties. Mock and coworkers reported the first fully chemical nature and structure of CB6 in 1981.[18] After the characterization of CB6, several efforts have been made to characterize CB5, CB7 and CB8 and these strategies were extended to discover CB[n] family.[20] Then CB10 was characterized by the Isaacs group.[21] Due to having large cavity, CB10 can bind large guest molecules such as calix[4]arene. CB[n] family has diverse applications in the different areas such as the design of rotaxanes and pseudorotaxanes, molecular machines and switches, drug delivery systems, switchable catalyses, water treatment and the extraction of amino acids.

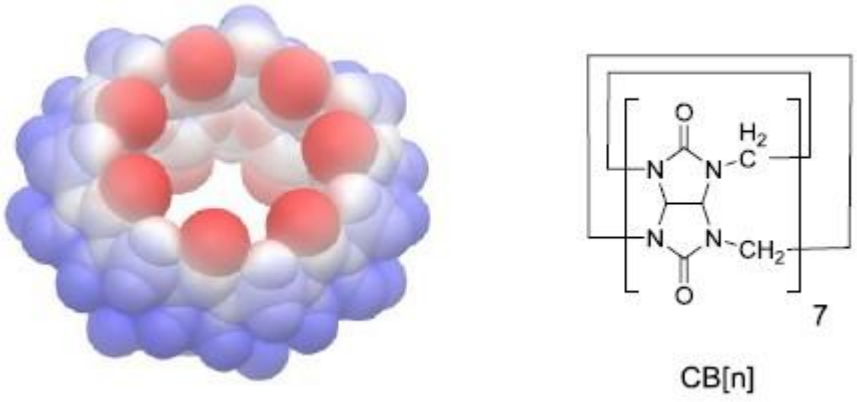

Figure 8. Representation of the electrostatic potential of CB7 (left side) and its molecular structure (right side).[22]

2.4.1. Synthesis, Structure and Chemical and Physical Properties of CB[n]

CB[n] compounds can be produced through an acid-catalyzed condensation reaction of glycouril and excess formaldehyde in the presence of concentrated sulfuric acid or hydrochloric acid at about 110 ^{o}C. As the number (*n*) increases, the cavity size also increases in the CB[n] family. Although CB[n]s demonstrate excellent host-guest

properties with a variety of host molecules, their low solubility in common solvents limits their usage.[23] Their solubility is fairly good in strongly acidic solution or in aqueous solutions containing alkali metal ions. However, due to having excellent water solubility and relatively large host cavity compared to the other CB analogs, CB7 is a promising candidate in the host-guest study applications.

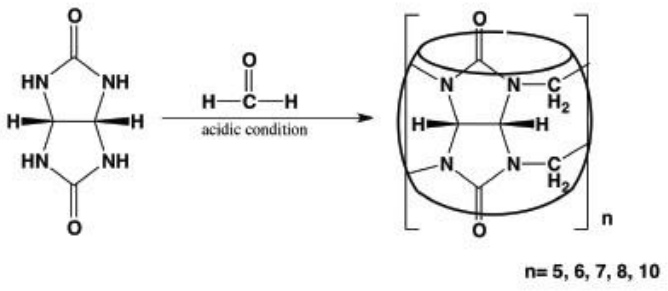

Figure 9. Synthesis of CB[n]s under acid-catalyzed condensation reaction.

2.4.2. Host Guest Properties of CB7

CB7 has great water solubility and its tendency to encapsulate aromatic species due to having larger cavity makes it easier to handle therefore it takes more attention during the past few years. It can form complexes with different hosts such as stilbenes[24], viologen dications[25], protonated aminoadamantanes[26], protonated polyaromatic amines[27], pyridinium derivatives[28].

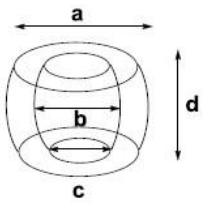

		CB5	CB6	CB7	CB8
Outer diameter (Å)	a	13.1	14.4	16.0	17.5
Cavity diameter (Å)	b	4.4	5.8	7.3	8.8
Portal diameter (Å)	c	2.4	3.9	5.4	6.9
Height (Å)	d	9.1	9.1	9.1	9.1

Figure 10. Molecular dimensions for CB[n] family members.

2.4.3. Cucurbit[n]uril Based Rotaxanes

Cucurbiturils seem more relevant with regards to molecular machine design, since they can form very stable complexes with a number of aromatic amines and quaternized pyridinium and viologen species.[29] There are exciting examples of molecular switches and machines built using these host species.[30] In recent years, Kim and coworkers have published several papers based on molecular shuttles with cucurbit[n]uril family. In one of them, kinetically controlled molecular machine was investigated.[30] This molecular machine was controlled with pH and switching from one station to another was controlled by the change in pH. However, the reverse process required not only pH change but also a thermal activation. The movement of CB6 from one station to another was provided with the deprotonation of the protonated diaminobutane. In order to drive the switching process, diisopropylethylamine was used to deprotonate the NH_2^+ group. Protonation was provided by an addition of strong acid, in this case DCl.

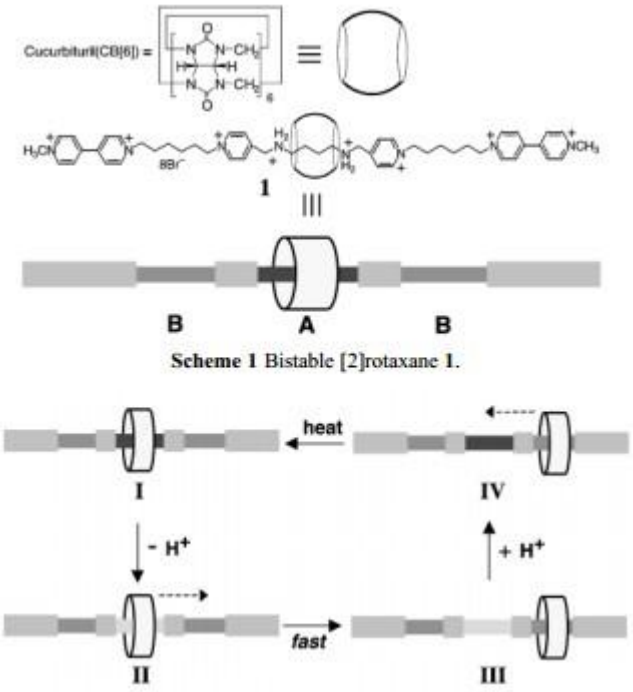

Figure 11. Switching cycle of bistable [2]rotaxane in the presence of CB6.[31]

2.5. Photophysical Methods

Photophysical methods are widely used during the last two decades in supramolecular chemistry. It offers numerous advantages with a high sensitivity in low concentrations. To deduce information from low concentrations is highly important phenomena. Receptor substrate association, formation and dissociation of supramolecular complexes have been investigated by photophysical methods. They are nondestructive methods and small amount of sample is required for the measurements. [32]

2.5.1. Fluoresence Signaling Phenomena

The most frequently used form of fluorescence modulation is the decrease or increase in fluoresence intensity at a single emission wavelength under the binding of analyte. PET (Photoinduced Electron Transfer) and PCT (Photoinduced Charge Transfer) are the most widely used concepts in supramolecular recognition which is explained in the following subsection. The fluorescence signaling phenomena was utilized in many areas such as molecular switches[33] and rotaxane based molecular machines.[34]

2.5.1.1. Photoinduced Electron Transfer (PET)

In the photoinduced electron transfer, electron jumps to another molecule or to part of a composite system as a result of absorption of light.[35] After the electron has jumped, a molecular ion pair is formed in the organic material, therefore an electron-hole pair is created. These ions and electron hole pairs recombine through radiative or non-radiative channels and they have a finite lifetime.

This kind of system contains a fluorophore which has a place of both photonic transactions of excitation and emission. A receptor molecule has a function of guest complexation and decomplexation. A spacer part is responsible for holding fluorophore and receptor close to each other.

In principle, photoinduced electron transfer (PET) can occur in two directions: from a donor to the excited-state fluorophore (reductive PET), or from an excited-state

fluorophore to a acceptor (oxidative PET). These both processes are combined with a quenching of the fluorophore emission.

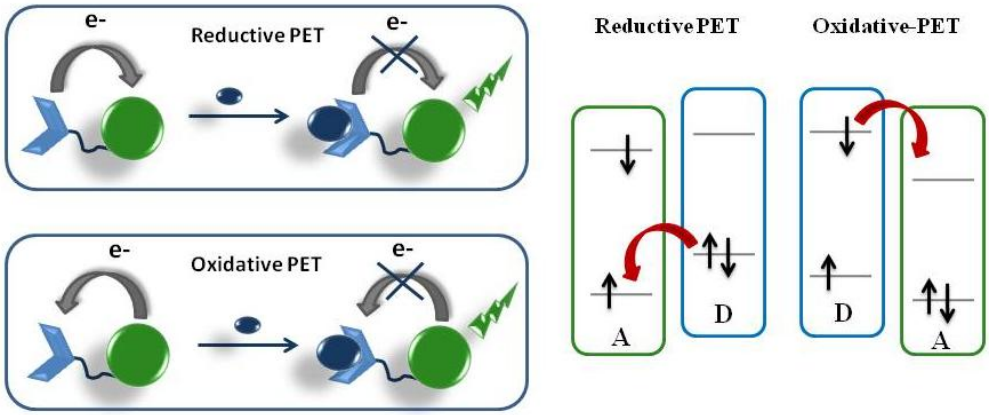

Figure 12. Cartoon representation of reductive and oxidative PET.

When fluorophore is excited, an electron transfer occurs from the HOMO of the donor to the HOMO of the receptor which is located under it. Therefore, the fluorescence is not observed. When cation binds to the recognition moiety, the energy of the HOMO level of the bound receptor decreases which is a result of the increase in the fluorescence. [36]

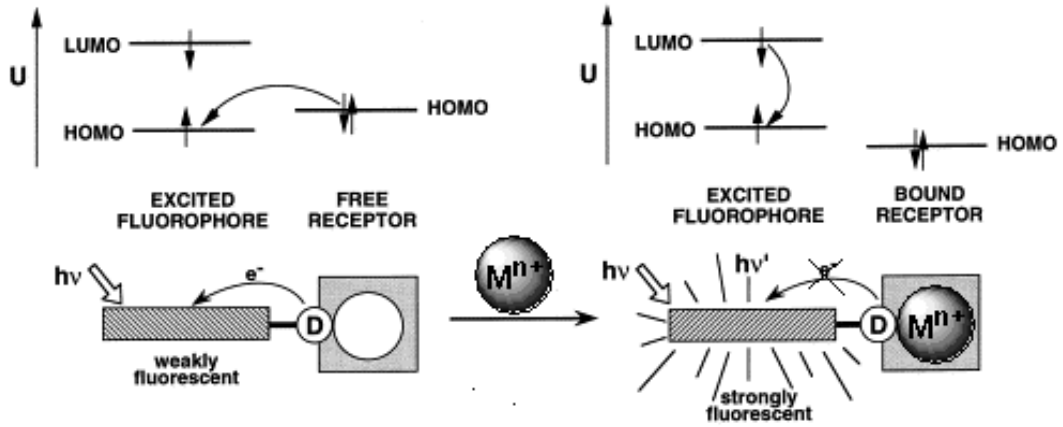

Figure 13. Schematical representation of PET mechanism.

When PET occurs from acceptor to donor, then it is called oxidative PET.[37]

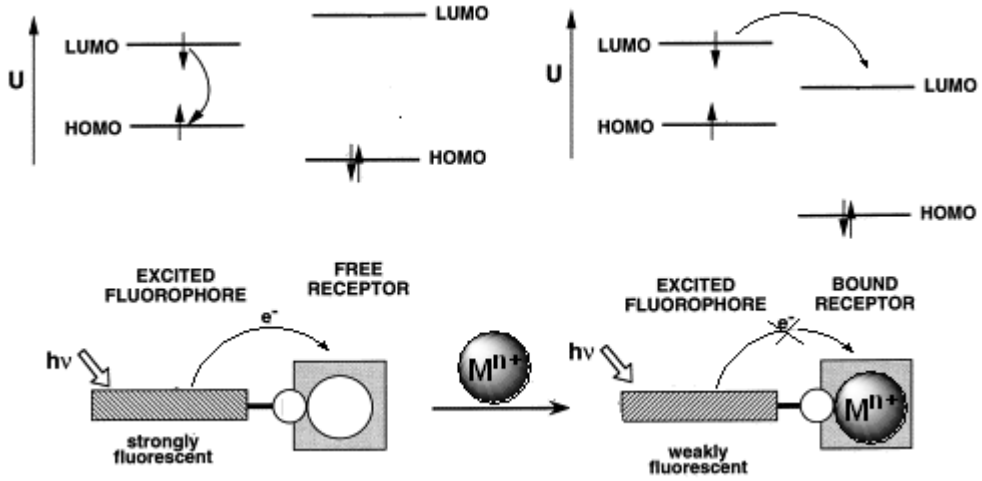

Figure 14. Schematical representation of oxidative PET mechanism.

In several cases, excitation energy transferred from the fluorophore after the prevention of PET by metal binding through ligand to another bound cation like Eu^{3+} or Tb^{3+}. Disappearance of emission signal from the fluorescent cations can be observed by this transfer. As an example of oxidative PET, the following work can be given which is studied by Akkaya *et al.* [38] In this study, fluorophore has bright-green fluorescence in the absence of zinc ion; however, the addition of zinc causes a quenching by oxidative PET mechanism.

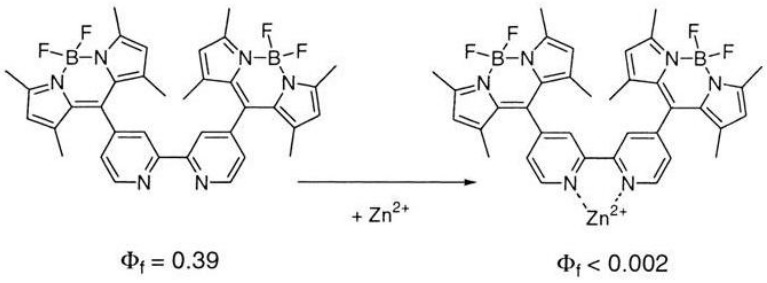

Figure 15. Complexation of zinc with bis-bipyridyl BODIPY fluorophore by oxidative PET mechanism.

2.5.1.2. Photoinduced Charge Transfer (PCT)

Intramolecular charge transfer from donor to acceptor occurs when a fluorophore contains an electron-donating group (generally an amino group) conjugated to an electron-withdrawing group upon excitation by light. Depending on the microenvironment of the fluorophore, resulting change in dipole moment reflects causes a Stokes shift. Photophysical properties of fluorophore change when cations are in close interaction with the donor or the acceptor moiety. Since the complex cation has an effect on the efficiency of intramolecular charge transfer. [39]

When an electron donor group (usually an amino group) within the fluorophore has a contact with a cation, the electron donating character of this group is reduced, and a blue shift of the absorption spectrum is observed with a decrease in the extinction coefficient. In contrast, when a cation interacting with the acceptor group improves the electron-withdrawing character of this group; therefore the absorption spectrum exhibits a red shift and the molar absorption coefficient is increased. In principle, the fluorescence spectra are shifted in the same direction with the absorption spectra. Changes in quantum yields and lifetimes are also observed as an addition of these shifts. These photophysical effects are based on the charge and the size of the cation.

When we focus only the case where the dipole moment in the excited state is larger than that in the ground state, as an interaction of cation with the donor group the excited state is more strongly destabilized by the cation than the ground state. Therefore, the blue shift of the absorption and emission spectra is expected. As a contrary, when the cation has an interaction with the acceptor group, the excited state is more stabilized by the cation than the ground state which results in a red shift in the absorption and emission spectra.

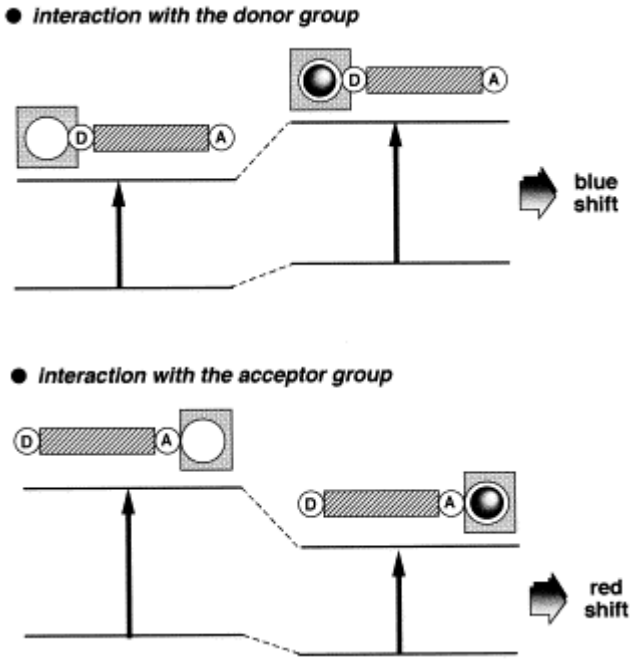

Figure 16. Spectral displacements of PCT sensors resulting from interaction of a bound cation with an electron-donating or electron-withdrawing group.

2.6. Oscillating Reactions and Their History

Oscillatory chemical reactions have been the subject of recent theoretical and experimental interest. Every living organism contains chemical oscillators. Therefore, the examinations of oscillating chemical reactions and nonlinear chemical dynamics have considerably more recent origins.

Oscillatory kinetics which is combined with surface reaction had been observed in 1828 by Fechner with an electrochemical system. Fechner proposed an electrochemical cell which produced an oscillating current. This work was the one which is published first about the oscillations in a chemical system. As an example of for these types of reactions, Figure 17 shows the variation of the potential at a Pt electrode with time for the electrochemical oxidation of H_2 in the presence of copper ions. While the potential at low–current density j is constant (a), at higher j kinetic oscillations occur because of periodic poisoning and activation transitions of the electrode by under potential deposition and dissolution of a passivating Cu overlayer. At first period doubling and then transition to an irregular situation (chaos) was observed with further increase of j.

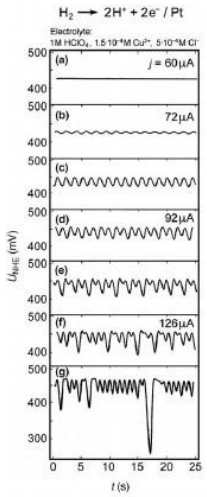

Figure 17. Time series of the potential of a Pt electrode during electrochemical oxidation of H_2 in the presence of copper ions at different current densities.

In 1899, Ostwald observed that the rate of chromium dissolution in acid increased and decreased periodically. Then, it is believed that homogeneous oscillating reactions were impossible since both systems were inhomogeneous. Belousov-Zhabotinsky reactions are perfectly fit into the rich variety of this type of temporal self-organization. After that, in 1970, the oscillatory kinetics was first reported combining with the heterogeneously catalyzed reactions for the oxidation of CO on Pt catalysts.

2.6.1. Lotka - Volterra Model

Alfred Lotka demonstrated a set of consecutive reactions can give rise to damped oscillations on the way to equilibrium. Vito Volterra used his ideas and tried to investigate a wide range of ecological problems, including the effects of migration and of several species simultaneously interacting. The well-known of this model is called the Lotka-Volterra model and it is often used to characterize the predator-prey interactions.

The Lotka-Volterra model consists of three irreversible steps. ***X*** represents the population of rabbits which reproduce autocatalytically. ***A*** represents the amount of grass and it has a constant value or can be considered as at least in great excess

compared with its consumption by the rabbits. ***Y*** is the population of lynxes (bobcats), and ***P*** stands for the dead lynxes.

$$\mathbf{A + X \rightarrow 2X}$$
$$\mathbf{X + Y \rightarrow 2Y}$$
$$\mathbf{Y \rightarrow P}$$

Each step is irreversible which corresponds to the fact that rabbits will never turn back into grass and dead lynxes will not turn back into the live ones. In order to describe the behavior of the predator and prey species the following differential equations can be written:

$$\mathbf{dx/\,dt = k_x ax - k_y xy}$$
$$\mathbf{dy/\,dt = k_y xy - k_d y}$$

k_x : rate constant represents how fast rabbits reproduce

k_y : rate constant represents how fast lynxes reproduce in a given number

k_d : rate constant which indicates the mortality rate of lynxes

The numbers of rabbits and lynxes will oscillate with a period that depends on k_x, k_y, k_d, and a for any set of these constants. The oscillatory populations of both species are coupled to each other with a certain phase shift. When the lynxes find enough food their population increases, while that of rabbits decays as soon as the birth rate cannot compensate the growing loss anymore. The oscillations in the two populations result from the difference in phases between rabbit reproduction and lynx reproduction. The rabbits reproduce because grass, *A*, is in constant supply. The lynx population will also increase, but only after the rabbit population has grown. Once the lynx population gets too high, since the grass supply is limited, rabbits will be eaten more rapidly than new rabbits are born, and their population will begin to decrease, which in turn will lead to a decrease in the lynx population. The rabbit population can then begin to rise again. Thus, there will be a time lag between the changes in the two populations. An approximate mathematical description of this effect can be achieved in terms of two coupled, nonlinear ordinary differential equations for the concentration of rabbits and lynxes together with the solution for properly chosen parameters k_x, k_y and k_d.

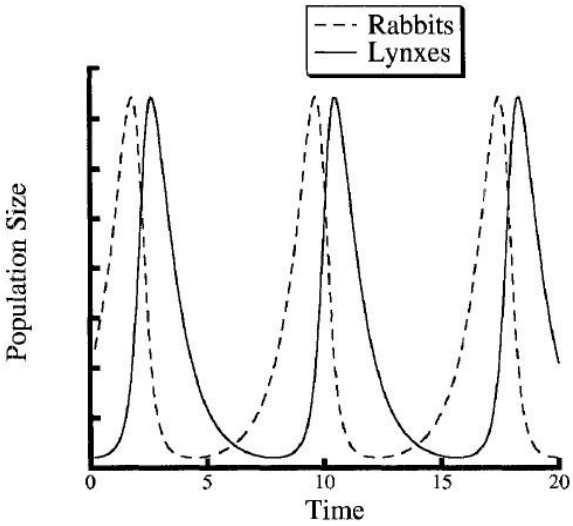

Figure 18. Numerical solution of the Votka- Volterra model w/ $A = k_x = k_y = k_d = 1$. (Oscillations in the rabbit and lynx population)[40]

2.6.2. Bray Reaction

Homogenous isothermal chemical oscillator was first investigated by William C. Bray[41] and it describes the reaction of iodate, iodine and hydrogen peroxide. Hydrogen peroxide decomposes into the oxygen and water. Under the catalytic conversion of hydrogen peroxide to oxygen and water in the presence of the iodate (IO_3^-), it is noticed that the rate of evolution of oxygen and the iodine (I_2) concentration were found to vary periodically.

First of all, hydrogen peroxide has a redox potential which provides the simultaneous oxidation of iodine to iodate which is indicated as the following:

$$5\ H_2O_2 + I_2 \rightarrow 2\ IO_3^- + 2\ H^+ + 4\ H_2O$$

Then the reduction of iodate back to iodine occurs and its reaction is demonstrated as the following:

$$5\ H_2O_2 + 2\ IO_3^- + 2\ H^+ \rightarrow I_2 + 5\ O_2 + 6\ H_2O$$

Depending on these two reactions, the system oscillates due to the concentration jump of the iodide and oxygen production. In this process the iodate catalysis of the disproportionation of hydrogen peroxide occurs. The net reaction is the following:

$$2H_2O_2 \rightarrow 2\ H_2O + O_2$$

2.6.3. The Belousov-Zhabotinsky Reaction

Russian biochemist Boris Pavlovich Belousov in 1950 discovered one of the most well- known oscillating reactions which is called Belousov- Zhabotinsky Reaction. It is one of the classes of reactions that serve as a classical example of non-equilibrium thermodynamics which results in the establishment of a nonlinear chemical oscillator. In these oscillating systems, the only common element is the inclusion of bromine and an acid. During these reactions, transition-metal ions catalyze oxidation of various reductants by bromic acid in acidic water solution. The Belousov-Zhabotinsky reactions show that chemical reactions do not have to be dominated by equilibrium thermodynamic behavior. They are far from the equilibrium and remain a significant length of time. Therefore, BZ reaction makes it amenable to observe the development of complex patterns in time and space by naked eye on a very convenient human timescale of dozens of seconds and space scale of several millimeters. For that regard, they provide an interesting chemical model of non-equilibrium biological phenomena and they can generate up to several thousand oscillatory cycles in a closed system.

He was trying to mimic the inorganic analog of Krebs cycle which is a key metabolic process in which citric acid was used as an intermediate. He investigated a solution of bromate, citric acid, and ceric ions (Ce^{4+}). He prepared a mixture which contains potassium bromated, cerium (IV) sulfate, propanedionic acid and citric acid in dilute sulfuric acid. He realized that the color of the solution oscillates between a yellow solution to colorless solution due to the ratio of concentration of cerium (IV) and cerium (III) ions oscillation. In this reaction mechanism, it is realized that cerium (IV) ions are reduced by propanedionic acid to cerium (III) ions and then they are oxidized back to cerium (IV) ions by bromate ions. In this experiment, ferrion was used as an indicator. It provides to improve the visual experience of the process since the ferrion reacts identically to the ceric ions and its relative concentration versus time graph would oscillate similar to that of ceric ion.

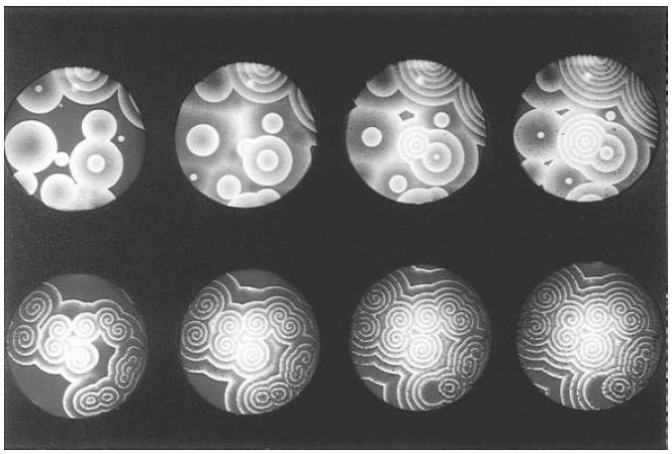

Figure 19. Target patterns and spiral waves in the Belousov-Zhabotinsky reaction observed in a Petri dish.[42]

2.6.4. The Briggs Raucher Oscillation Reaction

The visually striking oscillating reaction, the Briggs Raucher oscillation reaction, is developed by Thomas S. Briggs and Warren C. Rauscher. It is one of the most visually impressive chemical oscillations among the other oscillations.[43] During Briggs Rauscher oscillation experiment; one can observe 15 or more cycles in a stirred batch of solution of colorless, to amber, to blue-black, before ending as a blue-black mixture with the odor of iodine. The general meaning of the Bray-Liebhafsky (BL) and the Belousov- Zhabotinsky (BZ) was combined and the Briggs-Rausher reaction was formed as a hybrid of these two reactions. Briggs and Rauscher discovered that oscillations still occurred if certain other organic compounds were used. For example, citric acid was replaced by malonic acid and Mn(II) ions were used as a one electron transfer agent instead of cerium ions. In this manner, Briggs and Rauscher combined the hydrogen peroxide and iodate of the Bray-Liebhafsky (BL) reaction with the malonic acid and manganese ions of the Belousov-Zhabotinsky (BZ) reaction, and discovered the oscillating reaction that bears their name.

In the Briggs- Rauscher oscillating reaction, the evolution of oxygen and carbondioxide gases and the concentrations of iodine and iodide ions oscillate. When the concentration of iodide ions is low, iodine produced rapidly. As the concentration of iodine in the solution increases, the intensity of the dark yellow color improves. The concentration of I_2 increases as the production of I^- and these

ions react with iodine molecules and starch to form a blue-black complex. This complex contains the pentaiodide ion (I_5^-). During the formation of I_2, most of the O_2 and CO_2 are produced. The concentration of I_2 reaches a maximum and begins to fall, although the concentration of I^- rises further and remains high as the concentration of I_2 continues to decline until the solution becomes clear. After that, the concentration of I^- suddenly falls and the cycle begins. This cycle was observed in a number of times and it ends when a deep blue mixture was originated which is an indication of a liberation of iodine vapors.

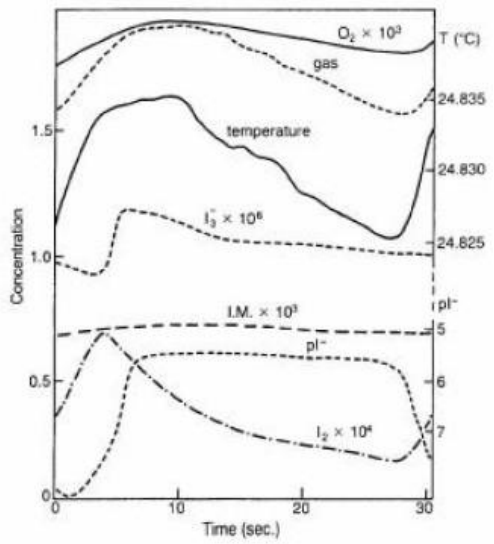

Figure 20. Variations with time of O_2, I_3^-, iodomalonic acid, and I_2 concentrations (in moles per liter), of pI-, of gas evolution (in arbitrary units), and of temperature (in Celcius) during one oscillation of Briggs-Rauscher reaction.[43]

The mechanism of Briggs- Raucher oscillating reaction explains the origin of oscillations in the concentrations of I_2 and I^-. According to the following reaction, the transformation which accounts for the oscillation can be deduced.

$$IO_3^- + 2H_2O_2 + CH_2(CO_2H)_2 + H^+ \rightarrow ICH(CO_2H)_2 + 2\ O_2 + 3\ H_2O \quad \textbf{(1)}$$

This transformation can be plausible with two component reactions.

$$IO_3^- + 2H_2O_2 + H^+ \rightarrow HOI + 2\ O_2 + 2\ H_2O \quad \textbf{(2)}$$

$$HOI + CH_2(CO_2H)_2 \rightarrow ICH(CO_2H)_2 + H_2O \quad \textbf{(3)}$$

First two reactions can occur via two different processes, a radical process and a nonradical process. Domination of these two reactions between each other depends on the concentration of iodide ions in the solution.

[I-] is low → the radical process dominates

[I-] is high → the nonradical process dominates

The last reaction combines the two processes. In this reaction, HOI is consumed more slowly than that species which is produced by the radical process under the conditions that this process is dominant. However, by the nonradical process HOI is consumed more rapidly than it is produced. The unreacted specie HOI after the reaction **(3)**, is reduced to I^- by hydrogenperoxide and it is one of the component steps of the nonradical process for the reaction **(2)**. When HOI is produced rapidly by the radical process, the excess forms of the iodide ions will not give permission for radical process and will slowly start the nonradical process. Then, depending on the reaction **(3)**, HOI is consumed more rapidly than that not enough HOI is available to produce the iodide ion necessary to keep the nonradical process going, and the radical process starts again. The reaction oscillates between these two processes since each of the processes of reaction **(2)** provides the conditions which leads to other process.

2.6.5. Some thermodynamical aspects

The Laws of thermodynamics can describe the behavior in the macroscopic scale of systems constituted of a great deal of microparticles. Most people who reject the existence of chemical oscillation based their refusal on the Second Law of Thermodynamics. The direction of spontaneous change can be predicted according to second law of thermodynamics. According to the second law:

$$\Delta S_{total} > 0 \quad \textbf{(4)}$$

where ΔS_{total} is the total entropy change of an isolated system or of the universe for the change of state of interest.

In chemical reactions, it is hard to determine the track of the entropy of the universe. If the reaction is performed under constant temperature and pressure, the requirement

which is indicated in equation **(4)** becomes equivalent to the requirement that the change in the Gibbs free energy be negative. There exists a function of state which depends only on the current condition of the system such as temperature, pressure, volume or concentration. This system is independent of its past history and it changes monotonically in any spontaneous process which provides to bring the system to its final equilibrium state.

People who object to the existence of oscillating reactions considered an oscillating reaction is analogous to a pendulum which passes through its equilibrium point during each cycle oscillation. Depending on this idea, they concluded that oscillation reactions make a contradiction with the Second Law since they would require the free energy of the system to oscillate as the reactants were converted to products and then back to reactants.

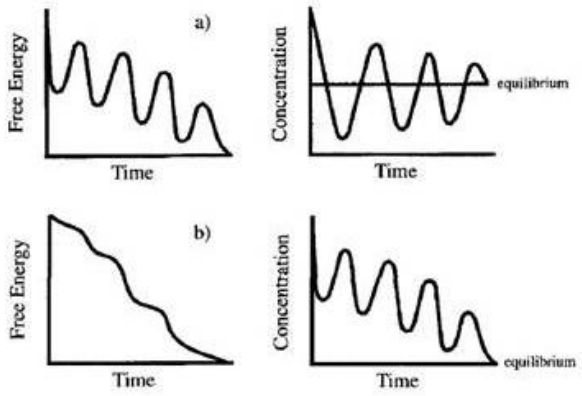

Figure 21. Two types of conceivable oscillations in closed systems, (a) oscillations around equilibrium; this is not consistent with the Second Law because the free energy must monotonically decrease to the equilibrium value, (b) oscillations on the way to equilibrium which is consisted with the Second Law.[44]

For chemical reaction systems operating under equilibrium or nearly equilibrium conditions, the steady state is unique which eliminates the possibility of multi-steady-state or oscillatory behavior under such conditions.

The formation of structures that are ordered in space and time seems to be at variance with the second law of thermodynamics; however all processes in a closed system without attractive interactions between the constituents tend to increase the entropy. Increasing entropy reflects itself in the increase of the grade of disorder. However,

chemical reactions at steady-state flow conditions occur in open systems where a constant flow of free energy keeps the system far away from the thermodynamic equilibrium. Therefore, such systems exhibit oscillatory or even chaotic behavior of the reaction rates. They also exhibit the formation of spatiotemporal concentration patterns.

2.6.6. pH Oscillation Reactions

Oscillating reactions[45] represent an interesting class of dynamic self-assembly. The archetypical Belousov-Zhabotinsky (BZ) reaction[46] behaves very well in closed systems, with large number of identifiable concentration peaks and troughs before the oscillations dampen. Unfortunately, necessity of Ce (III)-Ce (IV) couple limits the usage of Belousov-Zhabotinsky (BZ) reaction.

For that purpose, focusing on pH oscillations could be a choice.[47] There are only a few systems where pH oscillates in a controlled manner. Thiosulfate-sulfite-iodate is one of them, which displays high amplitude but irregular oscillations in batch systems.[48] In continuously stirred tank reactor (CSTR), oscillations are well behaved and essentially permanent, provided a steady supply of reactants and constant rate of removal for the products. Nevertheless, the batch system offered a solid potential for a proof of principle study.

All in all, oscillating reactions are among the most fascinating chemical reactions. These reactions are so fascinating to chemists since they seem to contradict the common sense. Under a given set of conditions, chemical reactions go in only one direction. According to the second law of thermodynamics, a chemical reaction reaches equilibrium and after that it cannot deviate from that condition spontaneously which is opposite to the oscillation phenomena. In order to exhibit oscillations, a chemical system must be far from its equilibrium composition.

Visually striking Briggs-Rauscher oscillation reaction and the Belousov-Zhabotinsky oscillation reaction are one of the most important oscillation experiments which were discovered at first and they lead to a promising research field in science. The Belousov- Zhabotinsky reaction is one of the classes of reactions which exhibits non-equilibrium thermodynamic behavior whereas the

Briggs- Rauscher oscillation reaction is the most visually chemical reaction among the other reactions in which one can observe 15 cycles or more during the oscillation experiment.

CHAPTER 3

3. EXPERIMENT RESULTS

3.1. General

Solvents used in synthesis were reagent grade. CH_2Cl_2, MeCN and Et_3N were used without further purification. Starting materials and reagents were purchased from Aldrich, Fluka, or Acros and used as received. All reactions were performed under an argon or nitrogen atmosphere and in dry solvents unless otherwise noted. Dry solvents were also purged with argon gas before using them. Reactions were monitored by analytical thin layer chromatography (TLC) using Merck TLC Silica gel 60 F_{254}. Chromatography on silica gel was performed over Merck Silica gel 60 (particle size: 0.040-0.063 mm, 230-400 mesh ASTM).

^{1}H NMR and ^{13}C NMR spectra were recorded at room temperature on Bruker DPX-400 (operating at 400 MHz for ^{1}H NMR and 100 MHz for ^{13}C NMR) at ambient temperature. Chemical shifts are reported in ppm relative to the signals corresponding to the residual non-deuterated solvents (D_2O: δ 4.79 ppm, CD_3OD: δ 3.31 ppm, $CDCl_3$: δ 7.26 ppm, DMSO-d_6: δ 2.50 ppm with tetramethylsilane (TMS) as internal standard). All spectra were recorded at 25^{o}C and coupling constants (*J values*) are given in Hz and chemical shifts are reported in parts per million (ppm). Splitting patterns are designated as singlet (*s*), doublet (*d*), triplet (*t*) and multiplet (*m*).

Absorption spectra in solution were acquired using a Varian Cary-100 spectrophotometer. Mass spectra were measured on an Agilent Technologies 6530 Accurate-Mass Q-TOF LC/MS spectrometer. Spectrophotometric grade solvents were used for spectroscopy experiments.

3.2. Syntheses

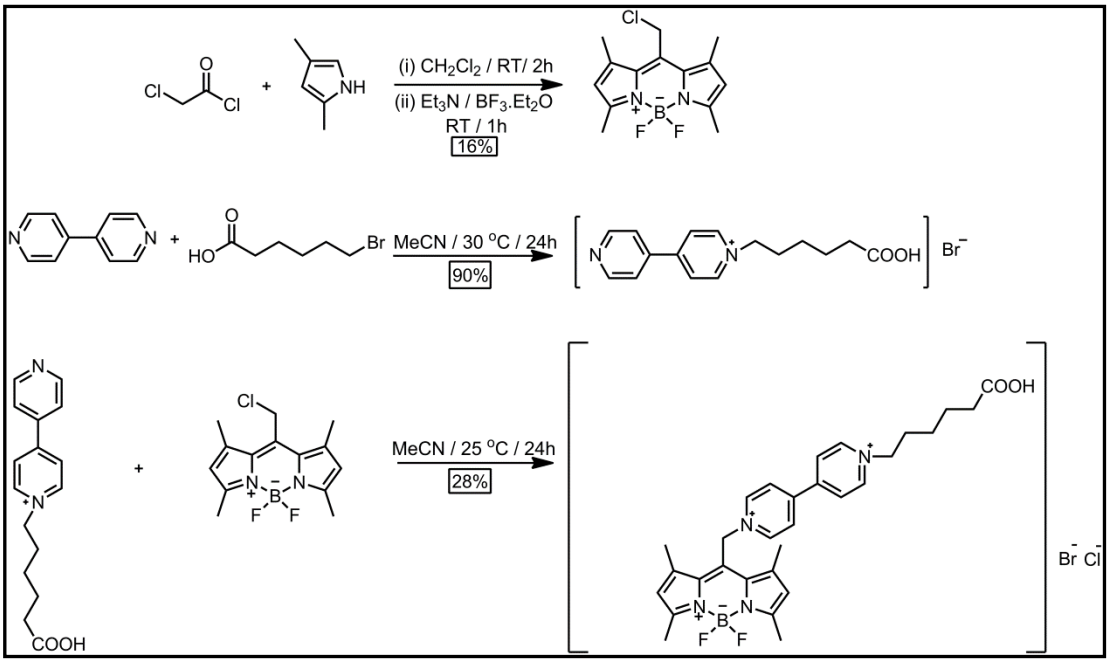

Figure 22. General reaction scheme for the target molecule.

3.2.1. Synthesis of 1

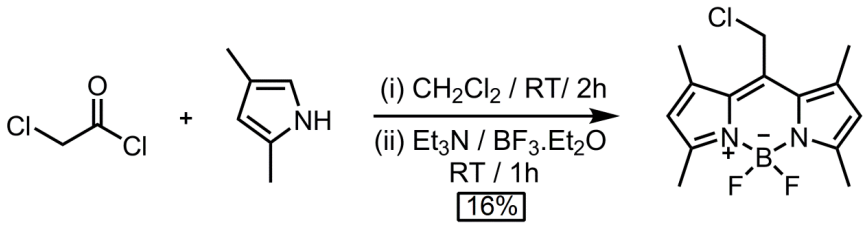

Figure 23. Synthesis of Compound 1.

To a 500 mL round-bottomed flask containing 250 mL argon-degassed CH_2Cl_2 were added 2,4-dimethyl-3-ethyl pyrrole (11.4 mmol, 1.5 g) and chloroacetyl chloride (5.7 mmol, 0.64 g) and the resulting mixture was stirred for 2 hours at room temperature. 8 mL of Et_3N and 10 mL of $BF_3.OEt_2$ were successively added and after 30 min, the reaction mixture was washed three times with water and carefully dried over anhydrous Na_2SO_4. The solvent was evaporated under reduced pressure to give the

crude product. Then, it was purified by using column chromatography (3:1 Toluene: Hexane) to give red solid (0.32 g, 16%).

^{1}H NMR (400 MHz, $CDCl_3$) δ = 6.03 (s, 2H), 4.71 (s, 2H), 2.47 (s, 6H), 2.46 (s, 6H).

^{13}C NMR (100 MHz, $CDCl_3$) δ = 156.63, 141.13, 135.92, 131.36, 129.04, 128.23, 122.30, 122.28, 37.17, 15.56, 14.72.

3.2.2. Synthesis of 2

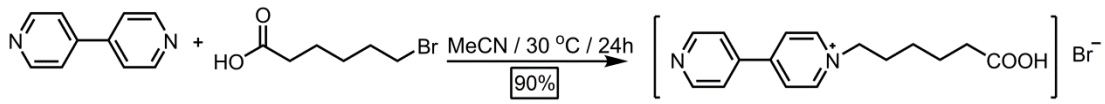

Figure 24. Synthesis of **Compound 2**.

4, 4'- Bipyridine (15.39 mmol, 2.4 g), 6-Bromohexanoic acid (15.13 mmol, 1g) and KI (5.13 mmol, 852 mg) were dissolved in pre-degassed MeCN (20 mL). The reaction mixture was stirred overnight at 30 °C. Cloudy solution was evaporated to 5 mL and the resulting suspension was added to 200 mL of diethyl ether to give the crude solid. Filtration and washing with 50 mL of diethyl ether yielded the product as pale yellow solids (1.2 g, 90%).

^{1}H NMR (400 MHz, D_2O) δ = 8.87 (d, *J* = 6.4 Hz, 2H), 8.69 (d, *J* = 5.2 Hz, 2H), 8.30 (d, *J* = 6.4 Hz, 2H), 7.92 (d, *J* = 5.7 Hz, 2H), 4.56 (t, *J* = 7.3 Hz, 2H), 2.22 (t, *J* = 7.3 Hz, 2H), 1.96 (p, *J* = 7.5 Hz, 2H), 1.52 (p, *J* = 7.4 Hz, 2H), 1.36 – 1.09 (m, 2H).

^{13}C NMR (100 MHz, D_2O) δ = 179.62 , 152.97 , 148.14 , 144.81 , 144.59 , 126.17, 123.26 , 61.39 , 34.11 , 30.11 , 24.65 , 23.78 .

MS (TOF- ESI): m/z: Calcd: 271.14410 , Found: 271.1441.

3.2.3. Synthesis of 3^{2+}

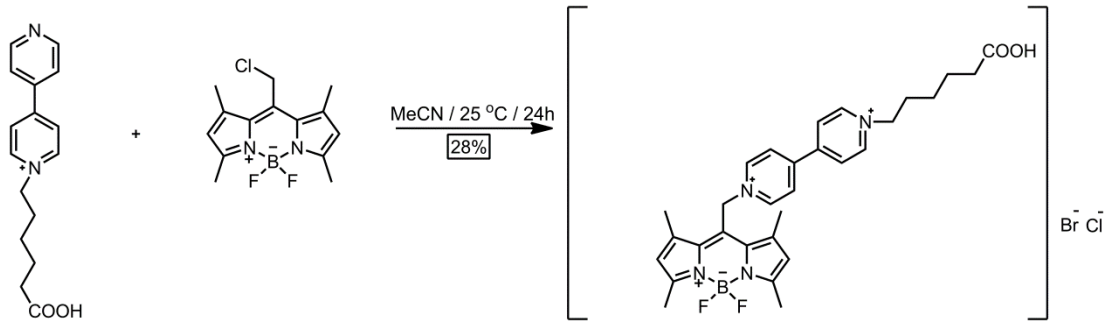

Figure 25. Synthesis of Compound $\mathbf{3}^{2+}$.

Compound **1** (0.33 mmol, 100 mg), compound **2** (0.67 mmol, 183 mg) and catalytic amount of KI were added to a 100 mL round-bottomed flask containing 30 mL pre-degassed MeCN. The reaction mixture was heated at 45 ^{o}C under argon atmosphere for overnight. The resulting red suspension was evaporated under reduced pressure until 5 mL of solvent remained in the round-bottomed flask. Then, this concentrated suspension was added to 200 mL of cold diethyl ether to give dark red solids. The filtrated solids were washed with diethyl ether extensively. The crude product was purified by alumina gel column chromatography (5:95 MeOH: $CHCl_3$) to give dark red solids (0.06 g, 28%).

^{1}H NMR (400 MHz, CD_3OD) δ = 9.09 (d, *J* = 6.9 Hz, 2H), 8.86 (d, *J* = 6.3 Hz, 2H), 8.53 (d, *J* = 6.9 Hz, 2H), 8.01 (d, *J* = 6.3 Hz, 2H), 6.20 (s, 2H), 5.42 (s, 2H), 4.65 (t, *J* = 7.6 Hz, 2H), 2.50 (t, *J* = 7.3 Hz, 2H), 2.48 (s, 6H), 2.42 (s, 6H), 2.07 (p, *J* = 7.7 Hz, 2H), 1.75 (p, *J* = 7.4 Hz, 2H), 1.56 – 1.39 (m, 2H).

^{13}C NMR (100 MHz, CD_3OD) δ = 174.29 , 157.61 , 155.14 , 151.84 , 146.49 , 143.62 , 143.41 , 135.71 , 133.76 , 127.13 , 123.55 , 123.27 , 62.39 , 58.85 , 34.32 , 31.96 , 26.51 , 25.29 , 15.79 , 14.66 .

MS (TOF- ESI): m/z: Calcd: 531.2732 $[M-H]^-$, Found: 531.2735 $[M-H]^-$.

CHAPTER 4

4. EVALUTION

Interlocked molecules such as rotaxanes are important components of molecular device design. Commonly, rotaxanes have two different stations which can be activated by external stimuli. The switching process can be investigated by the changes in NMR spectroscopy, absorption spectra and infrequently by emission changes. In this work, we tried to accomplish shuttling of the cucurbit[7]uril from one station to another by changing the pH from basic to acidic. The axle component of the pseudorotaxane system is a Bodipy derivative (Figure 27). Bodipy is a remarkable fluorophore with an amazing degree of versatility. [49] Under basic conditions, CB7 prefers to bind bipyridinium dication due to the ion-dipole interactions. However, under acidic conditions, carboxyl group is protonated and hydrogen bonding is more dominant than ion-dipole interactions and CB7 prefers to bind carboxyl group that is indicated in Figure 26. The shuttling of movement is investigated by the changes in emissive properties and NMR spectroscopy. At the end, this phenomenon is coupled to oscillation reactions to provide autonomous shuttling between the two stations.

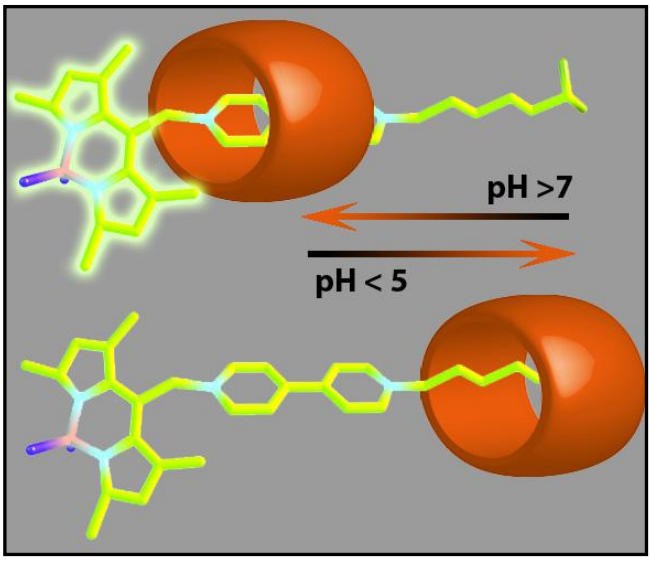

Figure 26. Schematical representation of our design.

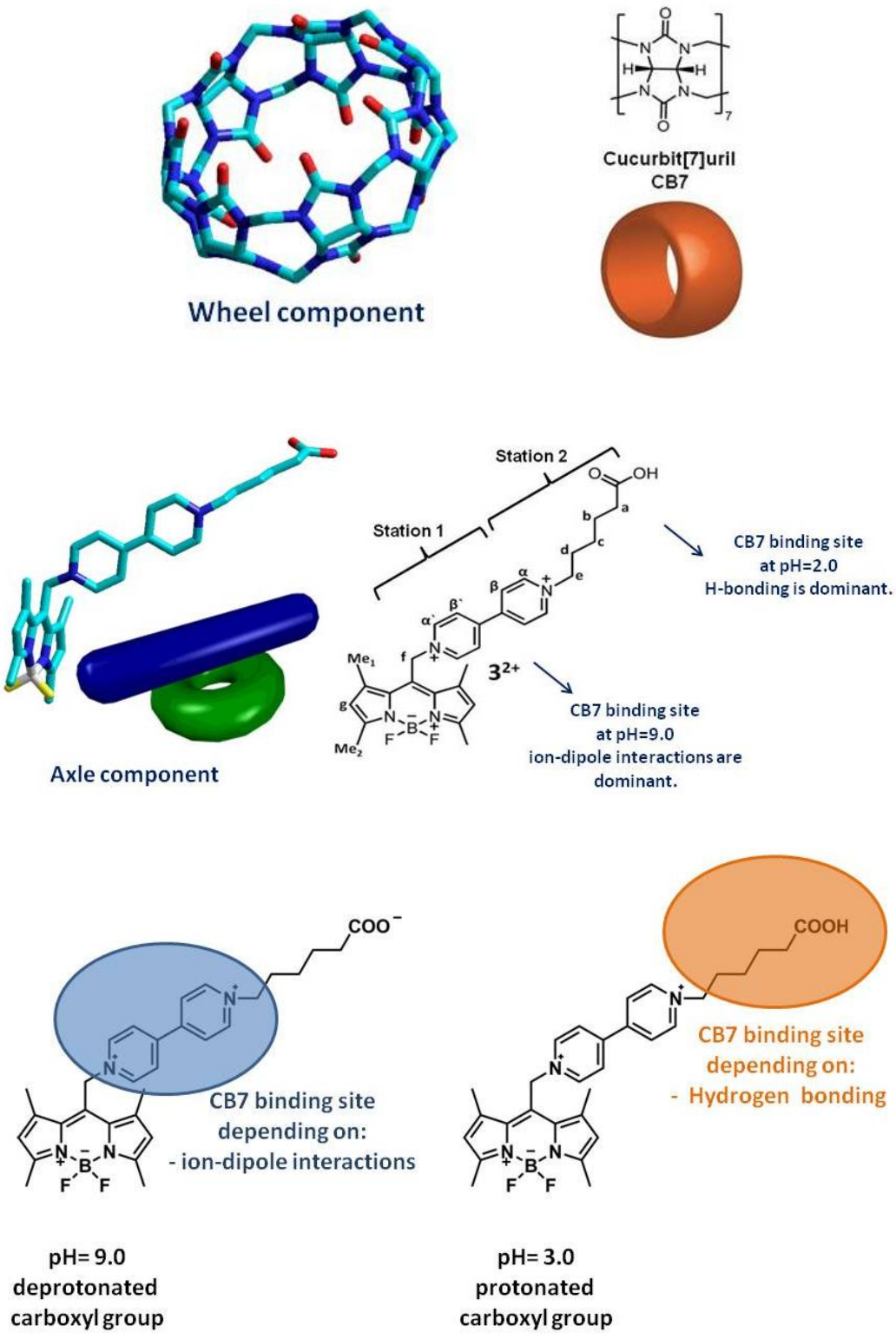

Figure 27. Structure of the fluorogenic 'axle unit' with two potential stations for CB7 and the 'wheel component'.

4.1. The Mechanism of Motion

Our previous work with the bipyridyl derivatives of BODIPY has shown that when complexed to Zn(II), bipyridyl LUMO energy level changes, allowing an oxidative or reverse PET (Photoinduced Electron Transfer) from the excited BODIPY unit, decreasing the intensity of emission. Later on, a systematic study of the relative frontier orbital energy levels of BODIPY and the *meso* substituents by Nagano proved our earlier suggestion. Thus, we expect that any interaction reducing the charge density on pyridinium moiety would increase the emission intensity as a result of decreased reverse (oxidative) PET. The rest of our design was built on the results obtained by Kaifer. Carboxylic acid functionality linked to a bipyridinium dication moiety with pentamethylene spacers were shown to offer two binding sites for CB7. It was shown by NMR studies that at neutral pH, CB7 prefers bipyridinium dication station, whereas under acidic conditions (when carboxylate group is protonated) carboxylic terminus becomes the preferred station. With these considerations in our design, we incorporated a carboxypentyl group as the second station. The BODIPY unit is the fluorescent reporter of the position of the wheel on the molecular axle, it is also a stopper, so at least from one end, CB7-$\mathbf{3}^{2+}$ complex is stoppered.

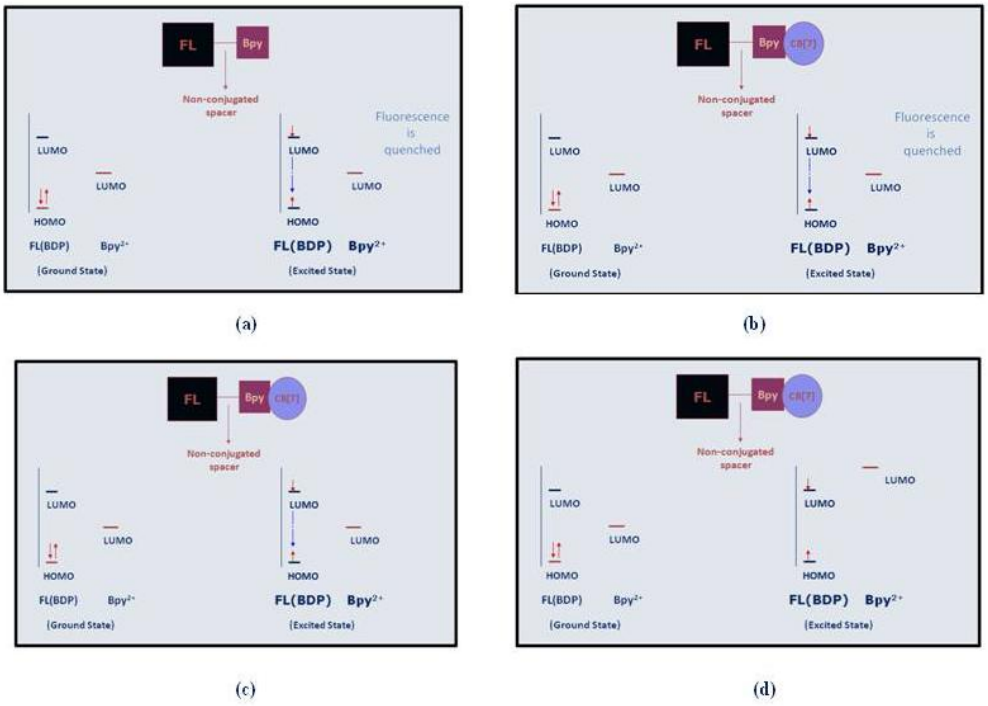

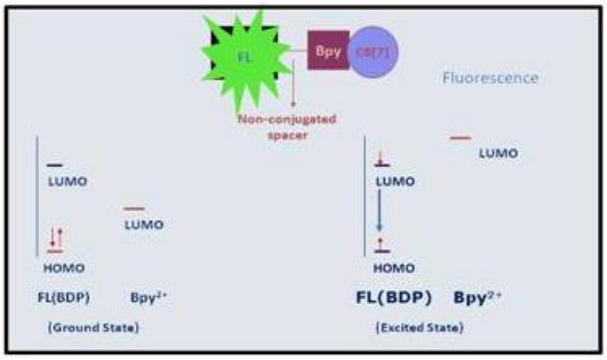

(e)

Figure 28. The cartoon representation of energy diagrams explaining oxidative PeT process.

4.2. Fluorescence Measurements

UV-Visible spectroscopy can be used under the guest absorbs light at different maximum wavelength values for the free and bound states. Very similar to NMR titrations, UV-Vis titrations carried out by changing the concentrations of host molecule (CB7).

The target Bodipy derivative has a reduced quantum yield as expected, reverse PET process competes effectively with the radiative deexcitation. The emission spectra of $\mathbf{3}^{2+}$ in the presence of increasing concentrations of CB7 are highly instructive (Figure 29). In the presence of CB7 at 10 μM (1.0 eq.), there is more than a fourfold increase in the emission intensity.

To further investigate the interaction of CB7 with $\mathbf{3}^{2+}$, we studied the changes induced by different concentrations of CB7 on the absorption spectra (Figure 30). The addition of CB7 to $\mathbf{3}^{2+}$ aqueous solution leads to an increase in the emission intensity, however, no shift of the absorption bands was observed. This suggests that the interaction of CB7 with $\mathbf{3}^{2+}$ does not lead to an important development of conjugated systems. The alteration in the ground state level is not observed therefore the absorption spectrum of the system is not affected.

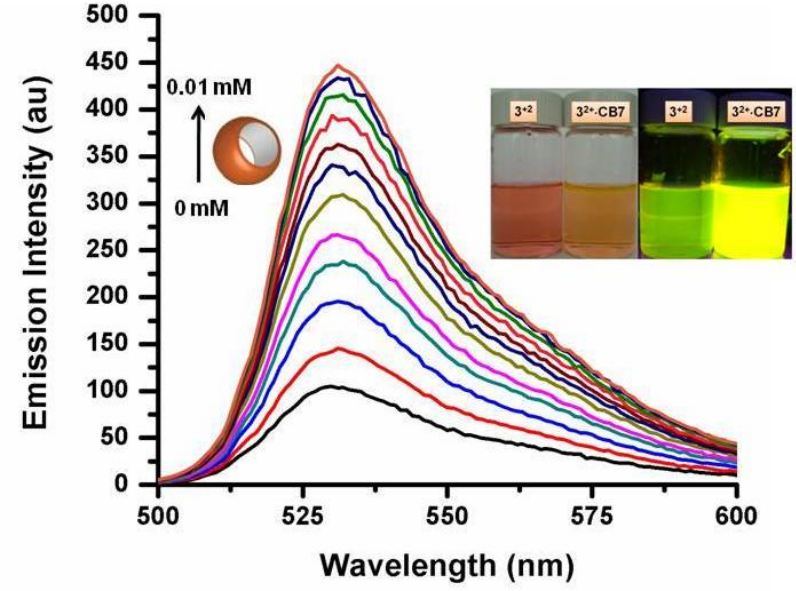

Figure 29. Emission spectra of compound $\mathbf{3}^{2+}$ (0.01 mM, in 0.1M NaCl 2% MeCN in D_2O) in the presence of increasing **CB7** concentrations (0, 0.1, 0.2, 0.3, 0.4, 0.5 0.6, 0.7, 0.8, 0.9, 1.0, 1.1 $x10^{-5}$M). The inset shows the appearance of solutions under ambient light (left) and under a hand-held 360 nm UV lamp (right).

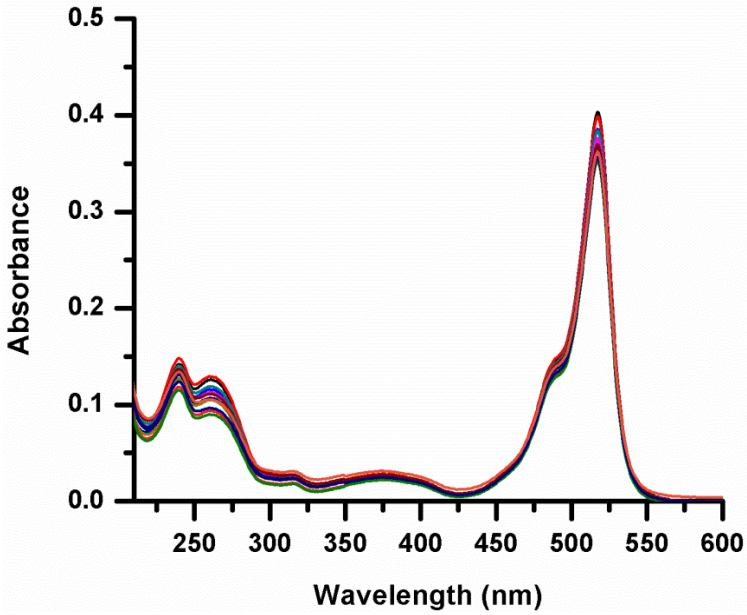

Figure 30. Absorption spectra of $\mathbf{3}^{2+}$ (0.01 mM in 0.1 M NaCl 2% MeCN in D_2O) in the presence of increasing concentration of CB7 (0, 0.1, 0.2, 0.3, 0.4, 0.5, 0.6, 0.7, 0.8, 0.9, 1.0, $1.1x10^{-5}$ M).

Figure 31 shows the pH directed reversible oscillations in emission spectra with the inclusion complex of $\mathbf{3}^{2+}$ and CB7 as monitored by switching pH between pH~2 and pH~9. As expected, the emission intensity is higher at neutral/alkaline pH, because when the CB7 moiety encapsulates bipyridinium dication (station 1), ion-dipole interactions partially neutralize the positive charge on the bipyridinium, slowing down reverse PET and allowing radiative transition to be the dominant mode of relaxation of the excited state. Thus, the spectra clearly show the switching of CB7 from one station to another when pH is changed from 9.0 to 2. It has to be pointed out that in the absence of CB7, emission spectrum of $\mathbf{3}^{2+}$ in aqueous medium shows essentially no dependence on pH in the range of interest (pH 2 to 9) which is indicated in Figure 32.

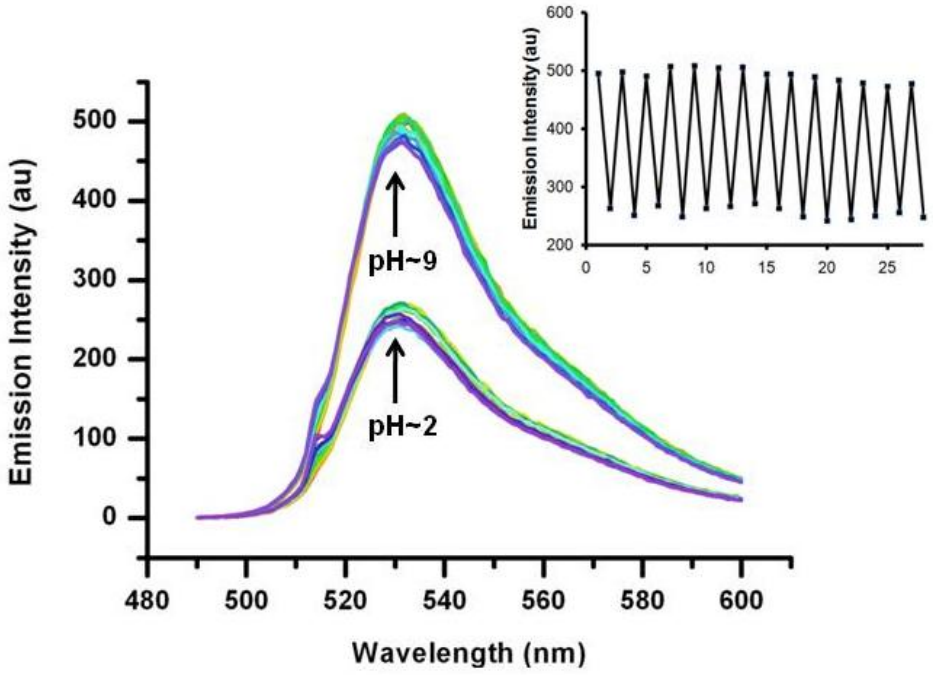

Figure 31. Emission spectra of solution compound $\mathbf{3}^{2+}$ (0.01 mM, in 0.1M NaCl 2% MeCN in D_2O) in the presence of 1.0 eq. CB7 cycled between pH~2 and pH~9. The inset shows emission versus pH~2 to pH~9 cycle recorded at 531 nm.

In separate control experiments without CB7, no change in the emission was observed, eliminating any possibility of chemical processes altering the Bodipy emission.

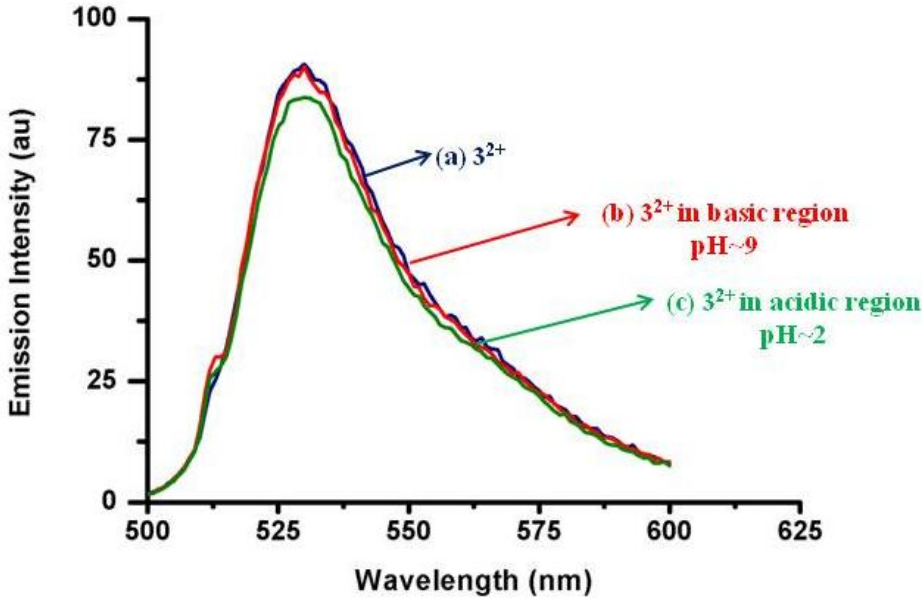

Figure 32. Emission spectra of (a) $\mathbf{3}^{2+}$ (0.01 mM, in 0.1 M NaCl 2% MeCN in D_2O) (b) in basic region (pH~9) (c) in acidic region (pH~2).

Then, control experiments were done in a time interval in the presence of CB7 in order to understand whether CB7 addition leads to a decomposition or not. According to our results, the emission spectra of $\mathbf{3}^{2+}$ both in basic and acidic region do not change during time which is an indication of the stability of the complex.

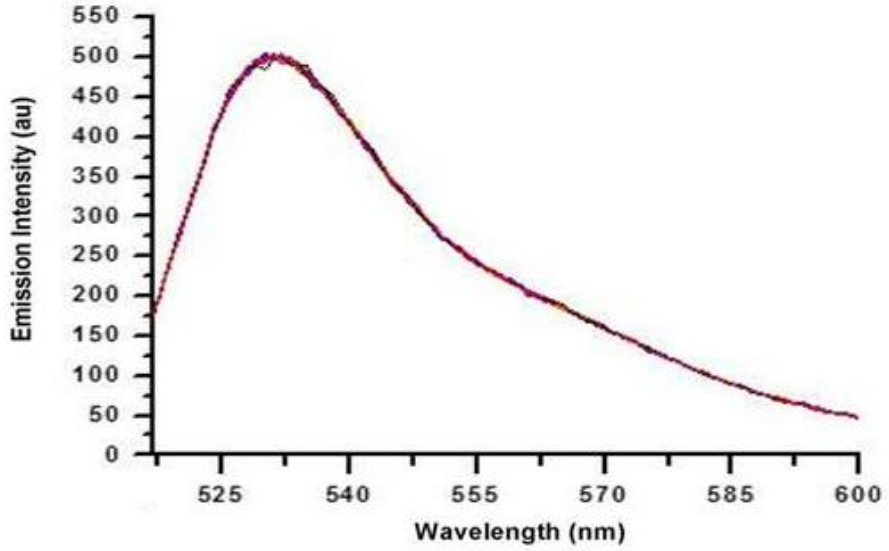

Figure 33. Emission spectra of compound $\mathbf{3}^{2+}$ (0.01 mM, in 0.1M NaCl 2% MeCN in D_2O) in the presence of 1.0 eq. CB7 with pH~8.

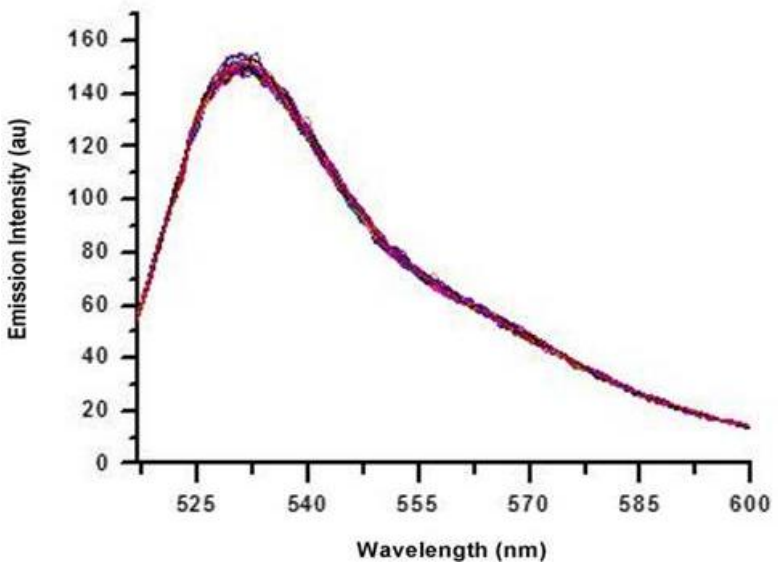

Figure 34. Emission spectra of compound $\mathbf{3}^{2+}$ (0.01 mM, in 0.1M NaCl 2% MeCN in D_2O) in the presence of 1.0 eq. CB7 with pH~3.

To investigate the emission intensity variation as a function of pH (Figure 35), 1:1 complex (the pseudorotaxane) was titrated in the pH range 9 to 1.6. When the pKa value of the carboxylic acid function is considered, the inflection point of the titration curve at pH 5 is in agreement with the literature data. Interestingly, the emission intensity of the complex is still higher than $\mathbf{3}^{2+}$.

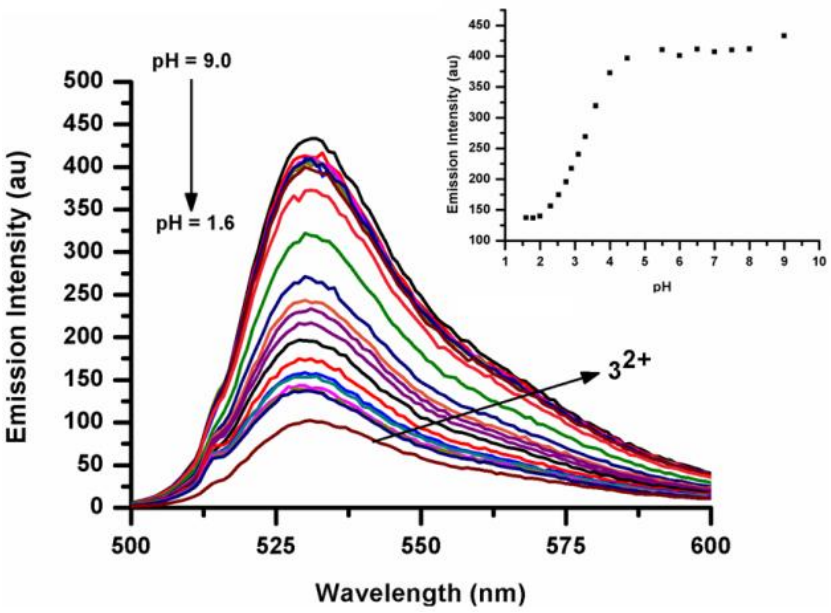

Figure 35. Emission spectra of compound $\mathbf{3}^{2+}$ (0.01 mM, in 0.1M NaCl 2% MeCN in D_2O) in the presence of 1.0 eq. CB7 with decreasing pH (9.0, 8.0, 7.5, 7.0, 6.5, 6.0, 5.5, 4.5, 4.0, 3.6, 3.3, 3.1, 2.9, 2.7, 2.5, 2.3, 2.0, 1.8, 1.6). Inset shows emission of $\mathbf{3}^{2+}$ complex as a function of pH recorded at 531nm.

4.3. NMR Studies

^{1}H NMR spectroscopy is a very practical and direct way in the determination of complex formation when the guest molecule is bound to CB7. It is also an extremely useful tool to find out information about the main binding site which is the main region of the guest capsulated into the CB7 cavity. Therefore, corresponding proton resonances demonstrate typically upfield shifts under the formation of complex. Similarly, the protons on the guest molecule which are located on the outside show downfield shifts in the complex although they are very close to the CB7 cavity portal. The information about the complexation behavior can be deduced from the observed chemical shifts (δ) of the guest protons in the absence and presence of the host molecule.

First of all, 2D-COSY NMR spectrum of compound $\mathbf{3}^{2+}$ was recorded in order to clarify the exact peak positions of protons. According to 2D-COSY NMR spectrum the place of the protons are labeled for the ease of detecting their shifts both in basic and acidic media. 2D-COSY NMR spectrum of $\mathbf{3}^{2+}$ showed that α' and β' protons are correlated whereas α and β protons are in close contact with each other. The more remote protons are also correlated in the NMR spectrum. Proton a and proton b are in close contact whereas proton b and proton c are located near each other. Moreover, proton d and proton c are correlated while proton d and proton e contact with each other. These interactions can be seen clearly in Figure 37, 38 and 39. At the end, labeled protons in the compound $\mathbf{3}^{2+}$ determined as the following:

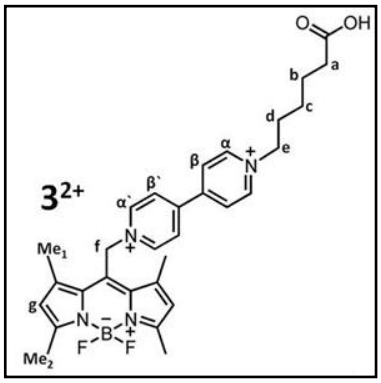

Figure 36. The labeled chemical structure of compound $\mathbf{3}^{2+}$.

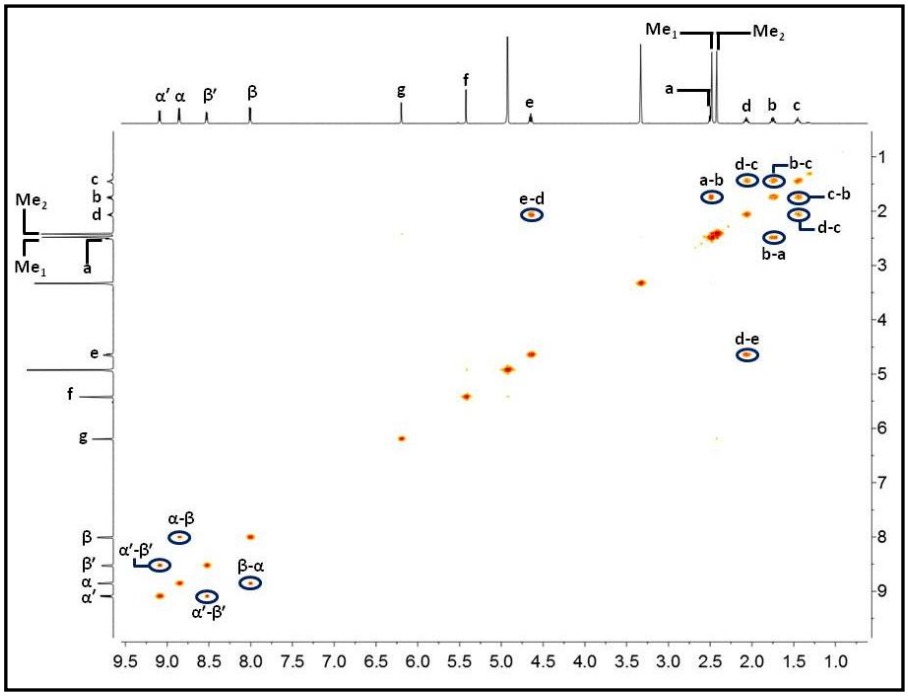

Figure 37. 2D-COSY NMR spectrum of $\mathbf{3}^{2+}$ recorded at 298K in CD_3OD.

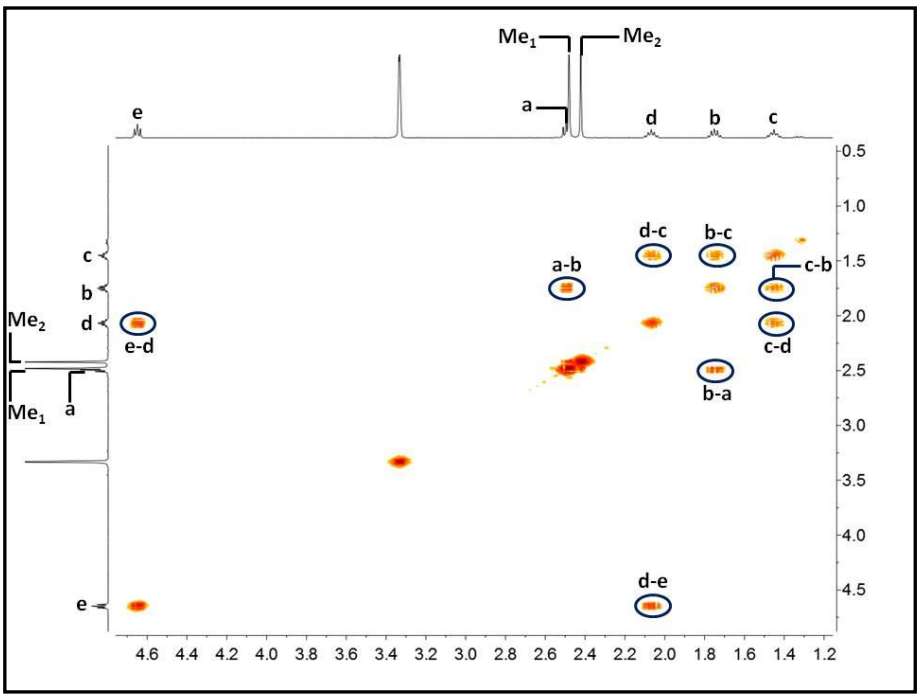

Figure 38. 2D-COSY NMR spectrum of $\mathbf{3}^{2+}$ recorded at 298K in CD_3OD (focused on aliphatic region).

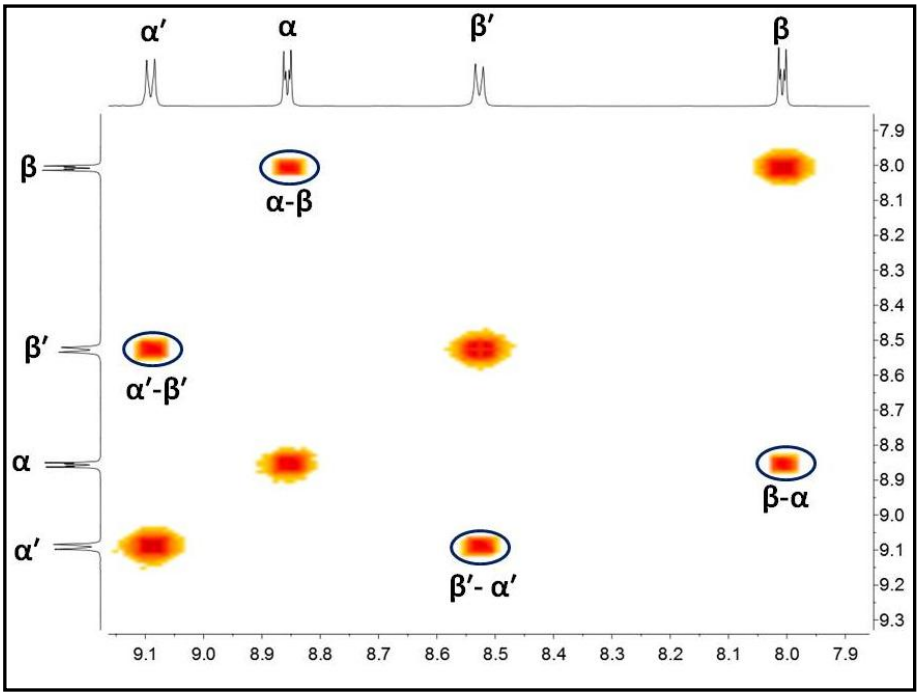

Figure 39. 2D-COSY NMR spectrum of $\mathbf{3}^{2+}$ recorded at 298K in CD_3OD (focused on aromatic region).

The interaction between $\mathbf{3}^{2+}$ and CB7 in slightly basic media was studied by ^{1}H-NMR spectroscopy. Figure 40 shows the titration experiment of $\mathbf{3}^{2+}$ (3 mM) with CB7 in 0.1 M NaCl / D_2O: CD_3OD (80: 20) solution (pD~8). As previously reported by Kaifer and Kim, the addition of 1.0 eq. CB7 resulted in an upfield shift of β and β' protons of viologen unit, by 0.80 and 1.18 ppm, respectively. Although the α proton, as expected, shows minor shift in the peak position (<0.1 ppm), the observed upfield shift for α' is 0.7 ppm. This reveals that in basic media, the Bodipy side of the viologen guest is pushed more into the cavity of CB7 which explains the unexpected large upfield displacement of the α' protons and also the different upfield shifts of β and β' protons. Because of this asymmetric arrangement within the pseudorotaxane, Me_1 and g protons interact with the carbonyl oxygens of CB7 portals and undergo a downfield shift. This interaction is also predominant in aliphatic region, especially e and d protons undergo a downfield shift. However, the more remote protons of the axle (a and b) are only slightly affected from the deshielding zone of the host and show a minor shift in peak positions. Furthermore,

this asymmetrical intrusion of viologen unit of the axle gives rise to splitting of CB7 protons.

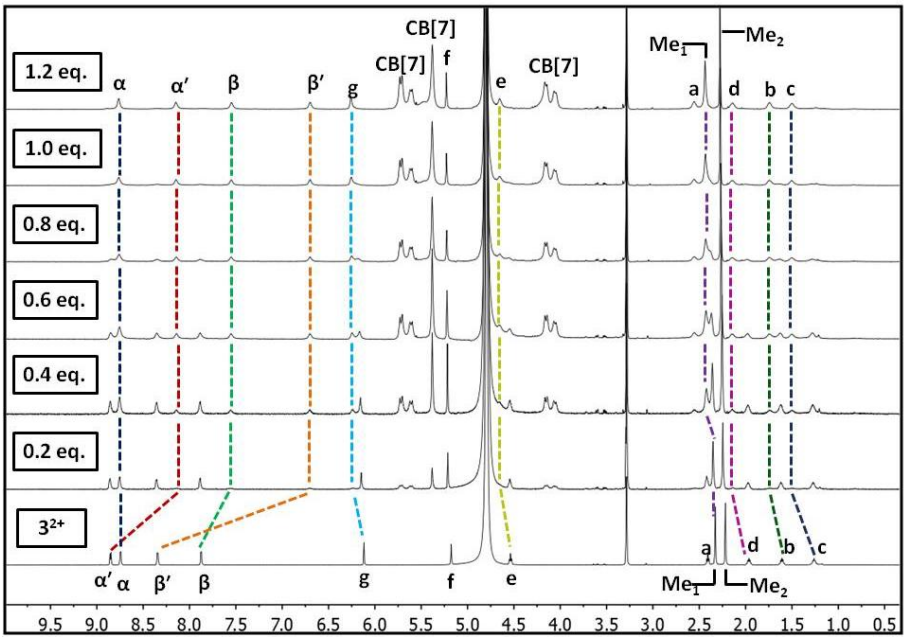

Figure 40. ^{1}H NMR titration spectra (400 MHz, 0.1 M NaCl in D_2O: CD_3OD; 70:30 at 25 ^{o}C) of $\mathbf{3}^{2+}$ (3.0 mM) in slightly basic media pH ~8 with increasing concentration of CB7 (0-1.2 eq).

The formation of inclusion complex between the guest ($\mathbf{3}^{2+}$) and host (CB7) molecules was also confirmed by 2D-COSY and 2D-NOESY NMR spectroscopy.

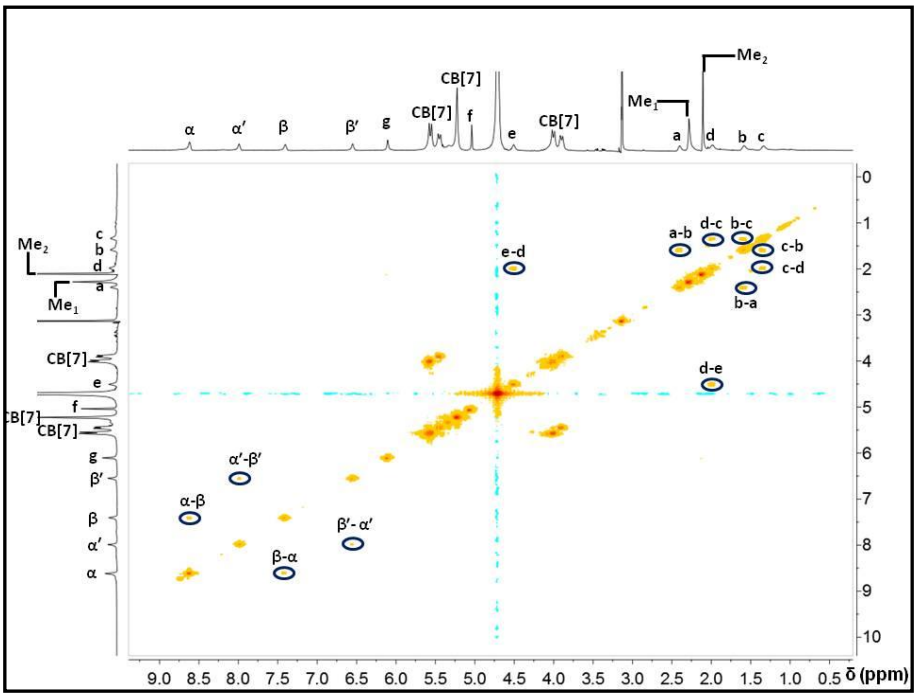

Figure 41. 2D COSY NMR spectrum of $\mathbf{3}^{2+}$ in presence of 1.2 eq CB7 in basic media pH~8 recorded at 298K in CD_3OD : D_2O (30 : 70).

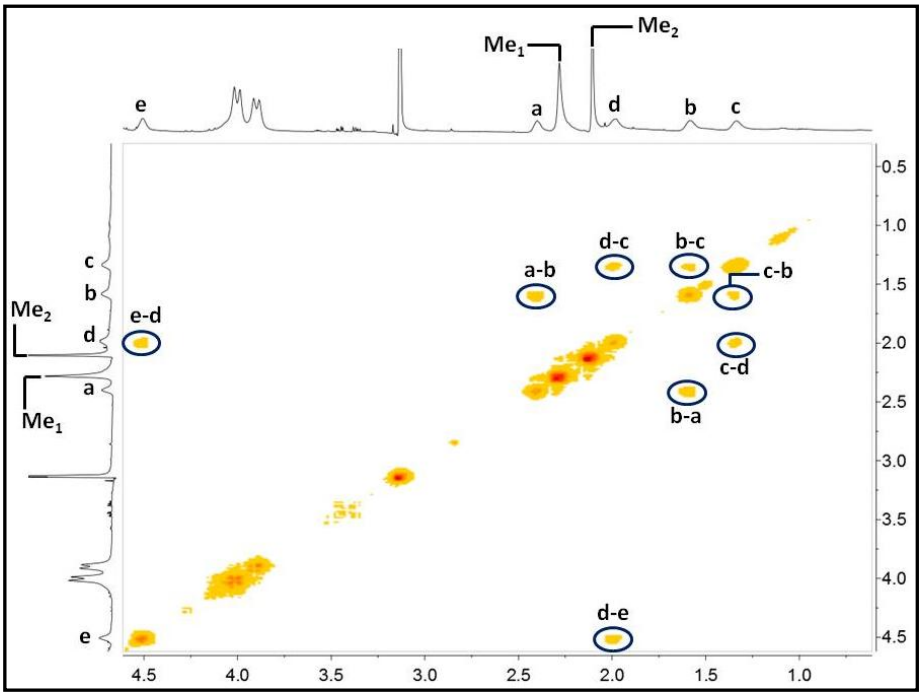

Figure 42. 2D COSY NMR spectrum of $\mathbf{3}^{2+}$ in presence of 1.2 eq CB7 in basic media pH~8 recorded at 298K in CD_3OD : D_2O (30 : 70) (focused on aliphatic region).

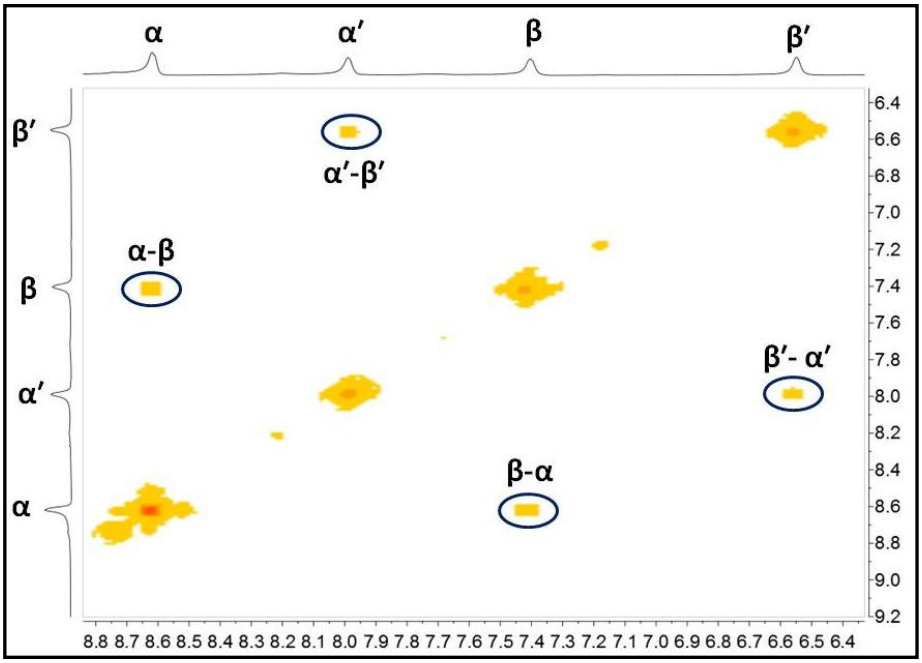

Figure 43. 2D COSY NMR spectrum of $\mathbf{3}^{2+}$ in presence of 1.2 eq CB7 in basic media pH~8 recorded at 298K in CD_3OD : D_2O (30 : 70) (focused on aromatic region).

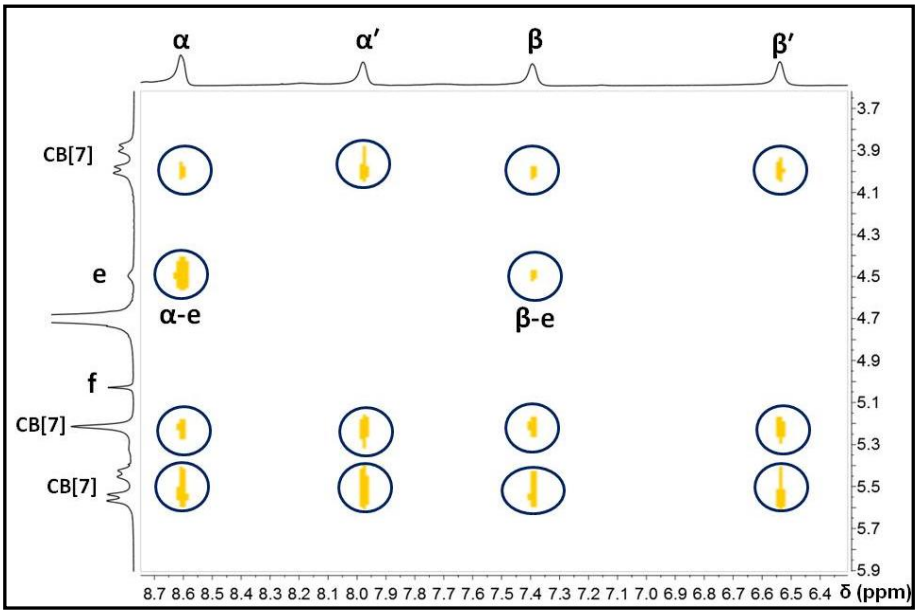

Figure 44. 2D NOESY NMR spectrum of $\mathbf{3}^{2+}$ in presence of 1.2 eq CB7 in basic media pH~8 recorded at 298K in CD_3OD : D_2O (30 : 70) (focused on aromatic region).

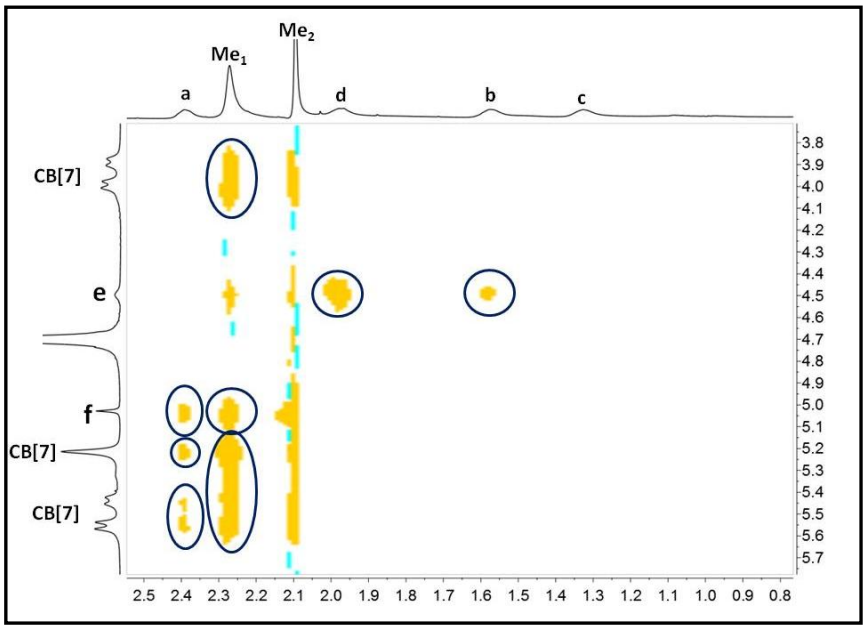

Figure 45. 2D NOESY NMR spectrum of $\mathbf{3}^{2+}$ in presence of 1.2 eq CB7 in basic media pH~8 recorded at 298K in CD_3OD : D_2O (30 : 70) (focused on aliphatic region).

In acidic media, concomitant to the reduction in emission intensity, (suggesting a preferential move away from the pyridinium cation immediately adjacent to the bodipy unit) 2D-NMR data show revealing changes. Methylene hydrogens show off-diagonal (cross peaks) with CB7 protons, a feature which does not show up in neutral/basic medium. β and β' protons are the most affected protons of the bipyridinium moiety in acidic media. In contrast, α and α' protons are not affected so much compared the β and β' protons. Thus, it is apparent that CB7 remains to be mostly bound to the Bodipy axle, yet it moves in the predicted direction.

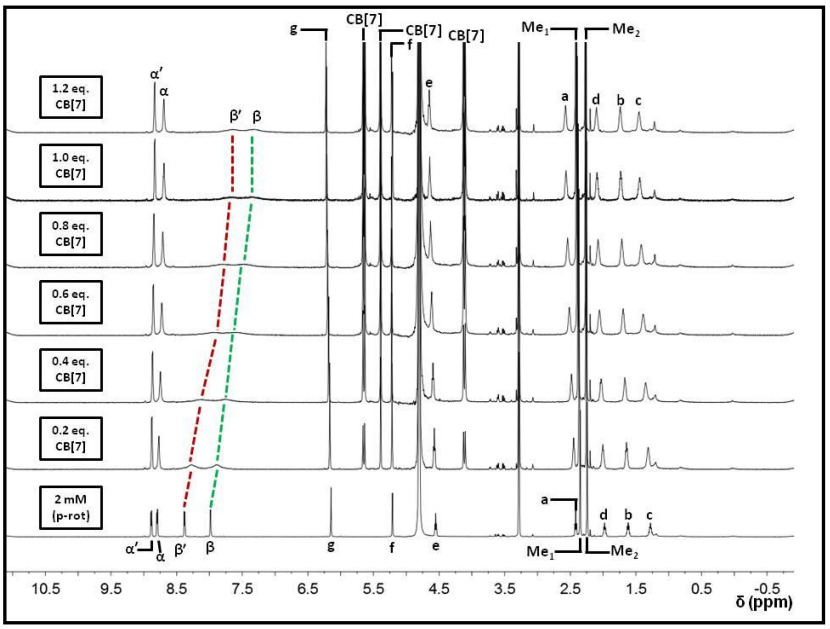

Figure 46. ^{1}H-NMR titration spectrum of $\mathbf{3}^{2+}$ with increasing concentration of CB7 (up to 1.2 eq) in acidic media (pH~3) recorded at 298K in CD_3OD : D_2O (30 : 70).

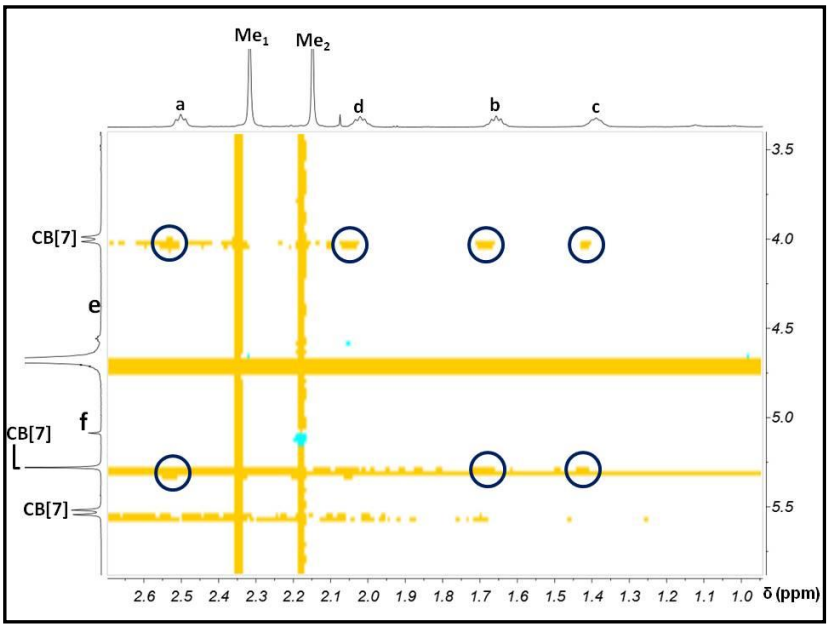

Figure 47. 2D NOESY NMR spectrum of $\mathbf{3}^{2+}$ in presence of 1.4 eq CB7 in acidic media (pH~3) recorded at 298K in CD_3OD : D_2O (30 : 70) (focused on aliphatic region).

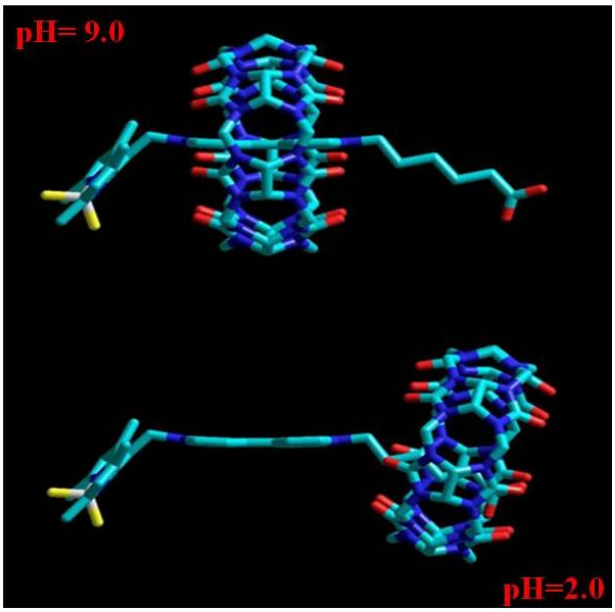

Figure 48 3-D Hyper-Chem drawings of pH switchable pseudorotaxane and wheel component under basic(pH=9.0) and acidic (pH=2.0) media.

4.4. Complexation Studies by Mass Spectroscopy

The formation of a stable inclusion complex between CB7 and $\mathbf{3}^{2+}$ was clear from MALDI-TOF mass spectroscopic data. The typical mass spectrum which shows the formation of the inclusion complex between viologen dication and CB7 is shown in Figure 49. Small peaks are evident at m/z 847.31 and 858.30, corresponding to doubly charged and doubly charged plus sodium ion 1:1 complexes of $\mathbf{3}^{2+}$ and CB7, respectively. However, the peak at m/z 847.31 $[3^{2+}\text{-CB7}]^{2+}$ is relatively more intense and the peak at m/z 858.30, the doubly charged plus sodium ion complex of $\mathbf{3}^{2+}$ and CB7, is the base peak. In summary, mass spectroscopy clearly shows the complexation of $\mathbf{3}^{2+}$ with CB7.

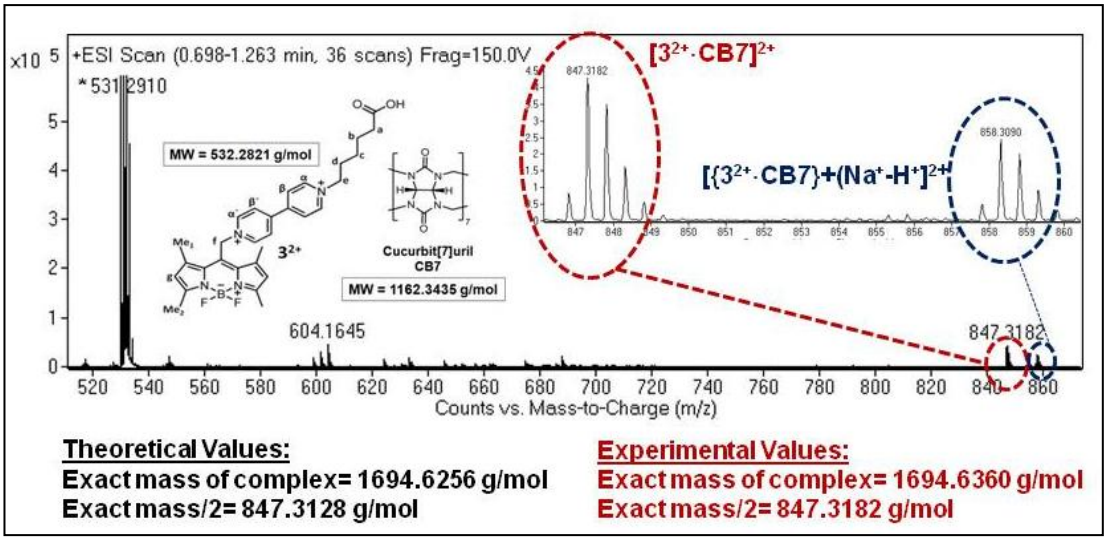

Figure 49. MASS spectrum of complex 3^{2+}·CB7.

4.5. Binding Constant Calculation

Equilibrium constant of the host-guest complex formation was determined from spectrophotometric titration data using Benesi-Hildebrand method. For that purpose, the titration curve of $\mathbf{3}^{2+}$ by CB7 was used. UV-Vis titrations of $\mathbf{3}^{2+}$ with increasing concentrations of CB7 give rise to plot composed of straight lines which intersect at a well-defined breaking point. These plots give information about complexation at absolute concentration levels and they are used for the calculation of binding constant. Fitting the absorbance data to the two simultaneous 1:1 binding gives the binding constant as 1.34 x 10^5 M^{-1} for the association of $\mathbf{3}^{2+}$ and CB7 which is indicated in Figure 50.

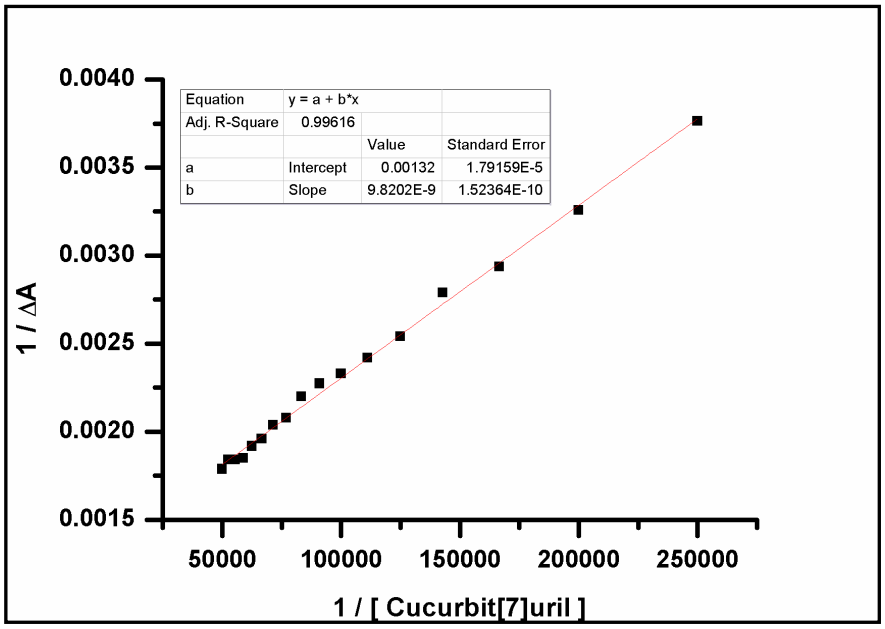

Figure 50. Benesi-Hildebrand analysis of compound $\mathbf{3}^{2+}$ at different CB7 concentrations.
Equation: y = a + bx, K = a/b = 1.34 x 10^5 M^{-1}

4.6. Oscillation Experiments

The very well documented process of shuttling in these systems almost always requires some sort of an external stimulus. We were motivated to offer an alternative and potentially autonomous mechanism by coupling the shuttling process to an oscillating chemical reaction. Once we established pH-mediated shuttling in aqueous solutions, we designed an experiment to realize similar shuttling in solution, but this time autonomously.

The archetypical Belousov-Zhabotinsky (BZ) reaction behave very well in closed systems, with large number of identifiable concentration peaks and troughs before the oscillations dampen. Unfortunately, we could not make use of Ce (III)-Ce(IV) couple. Metallo-catenanes/rotaxanes looked promising, but there has to be a match between the oscillation frequency and the switching rate between the two states. In most cases, switching back to the original states is much slower than what seemed appropriate. We then focused on aqueous systems and thus pH oscillations. We envisioned a situation where pH of a solution would be altered in a cyclic manner, switching the rotaxane between two bistable states. Thus, as long as the oscillation is sustained, the molecular machine would switch autonomously between these states. There are only a few systems where pH oscillates in a controlled manner. Thiosulfate-sulfite-iodate is one of them, which displays high amplitude but irregular oscillations in batch systems. In continuously stirred tank reactor (CSTR), oscillations are well behaved and essentially permanent, provided a steady supply of reactants and constant rate of removal for the products. Nevertheless, the batch system offered solid potential for a proof of principle study. Therefore, batch system in which pH oscillations for solutions containing thiosulfate, sulphite and iodate ions are well documented in the literature is utilized. For that purpose, we prepared thiosulfate (17.5 mM), sulphite (24.4 mM) and iodate (10 mM) solutions. The oscillations were started by the addition of 22 mM H_2SO_4 to yield a final concentration of 5.5 mM at the beginning of oscillation reaction. Concentration of CB7 (wheel) was 0.012 mM and the Bodipy derivative (axle) was 0.01 mM $\mathbf{3}^{2+}$.

In our hands, we observed a small decrease in pH by 0.1 units, and then a sharp drop of 3 pH units to nearly pH 2.4, and then oscillations die out, pH reaching a constant value. The changes are highly reproducible.

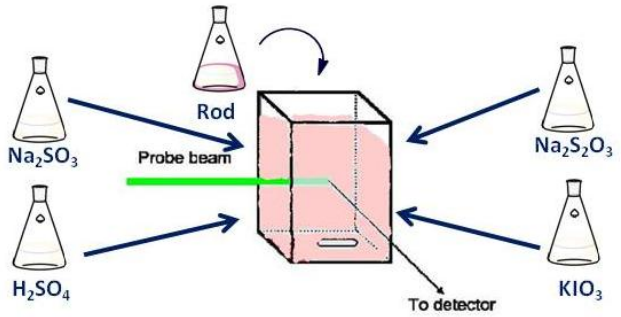

Figure 51. Schematic representation of oscillation experiment set-up.

To couple this oscillation to the shuttling of the pseudorotaxane, we carried out following experiments: in a fresh solution of the reagents, we added CB7 (0.012 mM) and 0.01 mM $\mathbf{3}^{2+}$. Oscillations were started by the addition of H_2SO_4 (5.5 mM) The switching was followed simultaneously by fluorescence spectroscopy and pH-meter: the first an 8% increase in the emission intensity, was observed, and at 360 seconds into the progression of the reaction, within a few seconds, a relatively fast drop (-84%) in the emission intensity was observed. The emission changes were reproducible, and juxtaposed very well with the changes in pH (Figure 52). The batch pH oscillations were highly irregular and only sustained for just one, or at most two cycles, nevertheless our results clearly serve as a proof of principle for autonomous switching in a pseudorotaxane through coupling to an oscillating reaction.

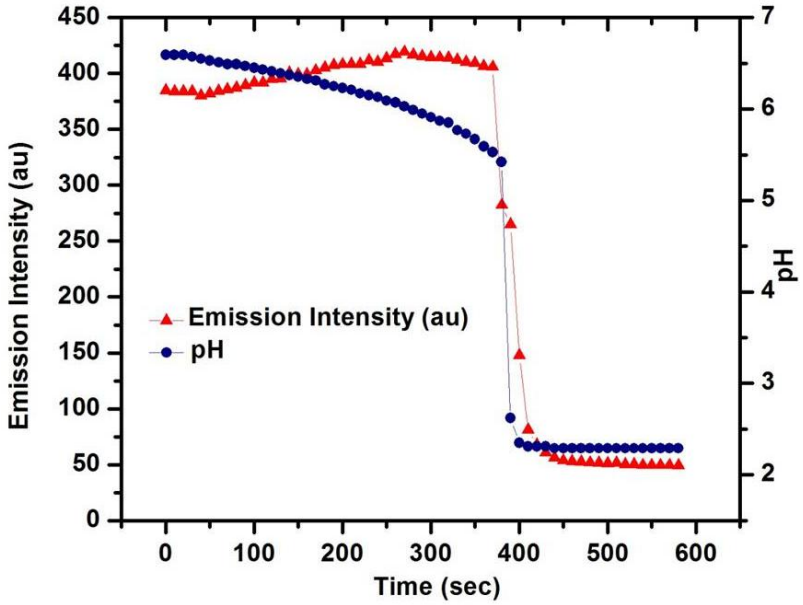

Figure 52. The plot of emission intensity and pH versus time obtained during the pH oscillation reaction coupled to the shuttling process.

CHAPTER 5

5. CONCLUSION

In this thesis, we proposed a novel and promising approach in the design of molecular machines. It is mainly focused on the development of a pseudorotaxane in which the shuttling of the cucurbit[7]uril (CB7) wheel is monitored by changes in the fluorescence of the BODIPY dye which is incorporated into the axle. Initiating molecular shuttling by oscillating reactions and controlling this shuttling were successfully achieved through a rational design. In the literature, the use of pH-dependent two-station axels containing the bipyridine moiety has been the subject of different studies dealing with rotaxanes based on benzo-crown, calixarenes, cyclodextrins, and even cucurbit[n]urils. However, this is the first example of such an axle containing BODIPY unit which changes its emission properties depending on the position of the wheel.

Even more interesting and novel of this project is the possibility of obtaining an independent shuttling of the wheel by coupling this system with an oscillating reaction, which causes wide pH changes. Therefore, this system yields a clear demonstration of shuttling in aqueous solution as a result of the protonation/deprotonation equilibrium of the carboxylic acid group incorporated into the pseudorotaxane structure. This approach is certainly rather interesting in terms of mimicking many biological analogs.

This is the rare demonstrations of a molecular shuttle system in which the “mobile” component is moving from one station to another in an autonomous fashion. When free energy of the oscillatory reactions is considered, the coupling of pH oscillation is clear. Therefore, it is exciting to combine this kind of chemical coupling of an energetically favorable reaction or set of reactions with complex kinetics to molecular motion. Since, in nature, there are so many examples which show oscillatory behavior. All in all, the proof of principle study described here, presents the first compelling evidence that oscillating reactions may provide such autonomy to molecular machines.

BIBLIOGRAPHY

1. Pedersen, C.J., 'The Discovery of Crown Ethers,' *Angew. Chem. Int. Ed. Engl.*, vol. 27, no. 8, pp. 1021-1027, 1988.

2. Cram, D.J., 'The Design of Molecular Hosts, Guests, and Their Complexes,' *Angew. Chem. Int. Ed. Engl.*, vol. 27, no. 8, pp. 1009-1020, 1988.

3. Lehn, J.-M., 'Supramolecular Chemistry—Scope and Perspectives Molecules, Supermolecules, and Molecular Devices,' *Angew. Chem. Int. Ed. Engl.*, vol. 27, no. 1, pp. 89-112, 1988.

4. **(a)** Balzani, V.; Credi A.; Venturi M., 'The Bottom-Up Approach to Molecular-Level Devices and Machines,' *Chem. Eur. J.*, vol. 8, no. 24, pp. 5524-5532, 2002.

(b) Balzani, V.; Credi A.; Venturi M., 'Molecular-Level Devices and Machines,' *Stimulating Concepts in Chemistry*, chapter 17.

5. Balzani, V.; Credi A.; Raymo M. F.; Stoddart F. J:, 'Artificial Molecular Machines,'*Angew. Chem., Int. Ed.* vol. 39, no. 19, pp. 3348-3391, 2000.

6. Balzani V., 'Nanoscience and nanotechnology: The bottom-up construction of molecular devices and machines,' *Pure and Applied Chemistry,* vol. 80, no. 8, pp. 1631–1650, 2008.

7. **(a)** Steed, J. W.; Atwood, J. L. *Supramolecular Chemistry*, Wiley: New York, 2000.

(b) Lindoy, L. F.; Atkinson, I. M. *Self-assembly in Supramolecular Systems* The Royal Society of Chemistry: Cambridge, 2000.

8. **(a)** Yamada, M.; Kondo, M.; Mamiya, J. I.; Yu, Y. L.; Kinoshita, M.; Barrett, C. J.; Ikeda, T., 'Photomobile Polymer Materials: Towards Light-Driven Plastic Motors,' *Angew. Chem.-Int. Edit.*, vol. 47, no. 27, pp. 4986–4988, 2008.

(b) Pease, A. R.; Jeppesen, J. O.; Stoddart, J. F.; Luo, Y.; Collier, C. P.; Heath, J., 'Switching Devices Based on Interlocked Molecules,' *R. Accounts of Chemical Research,* vol. 34, no. 6, pp. 433-444, 2001.

(c) Eelkema, R.; Pollard, M. M.; Vicario, J.; Katsonis, N.; Ramon, B. S.; Bastiaansen,C. W. M.; Broer, D. J.; Feringa, B. L., 'Molecular machines: Nanomotor rotates microscale objects,' *Nature,* vol. 440, pp. 163, 2006.

9. **(a)** Badjic, J. D.; Balzani, V.; Credi, A.; Silvi, S.; Stoddart, J. F., 'A Molecular Elevator,' *Science,* vol. 303, no. 5665 , pp. 1845-1849, 2004.

(b) Vella, S. J.; Tiburcio, J.; Loeb, S. J., 'Optically sensed, molecular shuttles driven by acid–base chemistry,' *Chem.Commun.,* vol. 45, pp. 4752-4754, 2007.

10. Deng, W. Q.; Flood, A. H.; Stoddart, J. F.; Goddard, W. A., 'An Electrochemical Color-Switchable RGB Dye: Tristable [2]Catenane,' *J. Am.Chem. Soc.,* vol. 127, no. 46, pp. 15994-15995, 2005.

11. **(a)** Brouwer, A. M.; Frochot, C.; Gatti, F. G.; Leigh, D. A.; Mottier, L.; Paolucci, F.; Roffia, S.; Wurpel, G. W. H., 'Photoinduction of Fast, Reversible Translational Motion in a Hydrogen-Bonded Molecular Shuttle,' *Science,* vol. 291, no. 5511, pp. 2124-2128, 2001.

(b) Saha, S.; Stoddart, J. F., 'Photo-driven molecular devices,' *Chem. Soc. Rev.,* vol. 36, no. 1, pp. 77-92, 2007.

12. **(a)** Coskun, A.; Banaszak, M.; Astumian, R. D.; Stoddart, J. F.; Grzybowski, B. A.,' Great expectations: can artificial molecular machines deliver on their promise?,'*Chem. Soc. Rev.,* vol. 41, no. 1, pp. 19-30, 2012.

(b) Wang, J. B.; Feringa, B. L.,' Dynamic Control of Chiral Space in a Catalytic Asymmetric Reaction Using a Molecular Motor,' *Science,* vol. 331, no. 6023, pp. 1429-1432, 2011.

(c) Hess, H.; Dumont, E. L. P., 'Fatigue Failure and Molecular Machine Design,' *Small,* vol. 7, no. 12, pp. 1619-1623, 2011.

(d) Gong, H. Y.; Rambo, B. M.; Karnas, E.; Lynch, V. M.; Keller, K. M.; Sessler, J. L., 'Environmentally Responsive Threading, Dethreading, and Fixation of Anion-Induced Pseudorotaxanes,' *J. Am. Chem. Soc.*, vol. 133, no. 5, pp. 1526-1533, 2011.

13. Balzani V.; Venturi M.; Credi A., *Molecular Devices and Machines*. VCH, Weinheim, 2003.

14. Ashton, P. R.; Ballardini R.; Balzani V.; Baxter I.; Credi A.; Fyfe C. T. M.; Gandolfi M. T.; Gómez-López M.; Martínez-Díaz V.; Piersanti A.; Spencer N.; Stoddart J. F.; Venturi M.; White J. P. A.; Williams D. J., 'Acid−Base Controllable Molecular Shuttles,' *J. Am. Chem. Soc.*, vol. 120, no. 46, pp. 11932-11942, 1988.

15. Balzani, V.; Leon M. C.; Credi A.; Lowe N. J.; Badjic D. J.; Stoddart J. F.; Williams D. J., 'Controlling Multivalent Interactions in Triply-Threaded Two Component Superbundles,' *Chem. Eur. J.* , vol. 9, no. 21, pp. 5348-5360, 2003.

16. Ashton P. R.; Ballardini R.; Balzani V.; Credi A.; Dress K. R.; Ishow E.; Kleverlaan J. C.; Kocian O.; Preece J. A.; Spencer N.; Stoddart J. F., Venturi M.; Wenger S., 'Photochemically Driven Molecular-Level Abacus,' *Chemistry - A European Journal*, vol. 6, no. 19, pp. 3558-3574, 2000.

17. Balzani, V.; Clemente-León M.; Credi A.; Ferrer B.; Venturi M.; Flood A. H.; Stoddart J. F., 'Autonomous artificial nanomotor powered by sunlight,'*Proc. Natl. Acad. Sci.*, vol. 103, no. 5, pp. 1178-1183, 2006.

18. **(a)** Masson, E.; Ling, X. X.; Joseph, R.; Kyeremeh-Mensah, L.; Lu, X. Y., 'Cucurbituril chemistry: a tale of supramolecular success,' *RSC Adv.*, vol. 2, no. 4, pp. 1213-1247, 2012.

(b) Lee, J. W.; Samal, S.; Selvapalam, N.; Kim, H. J.; Kim, K., 'Cucurbituril Homologues and Derivatives: New Opportunities in Supramolecular Chemistry,' *Accounts of Chemical Research*, vol. 36, no. 8, pp. 621-630, 2003.

(c) Nau, W. M.; Scherman, O. A., 'The World of Cucurbiturils — From Peculiarity to Commodity,' *Isr. J. Chem.*, vol. 51, no. 5-6, pp. 492-494, 2011.

19. Freeman, W. A.; Mock, W. L.; Shih, N. Y., 'Cucurbituril,' *J. Am. Chem. Soc.*, vol. 103, no. 24, pp. 7367-7368, 1981.

20. **(a)** Kim, J.; Jung, I. S.; Kim, S. Y.; Lee, E.; Kang, J. K.; Sakamoto, S.; Yamaguchi, K.; Kim, K., 'New Cucurbituril Homologues: Syntheses, Isolation, Characterization, and X-ray Crystal Structures of Cucurbit[n]uril (n = 5, 7, and 8),' *J. Am. Chem. Soc.*, vol. 122, no. 3, pp. 540-541, 2000.

21. Liu, S. M.; Zavalij, P. Y.; Isaacs, L., 'Cucurbit[10]uril,' *J. Am. Chem. Soc.*, vol. 127, no. 48, pp. 16798-16799, 2005.

22. Samir Andersson, ,'Supramolecular chemistry based on redox-active components and cucurbit[n]urils,' pp.2, 2010.

23. Lagona, J.; Mukhopadhyay, P.; Chakrabarti, S.; Isaacs, L.,' The Cucurbit[n]uril Family,' *Angew. Chem.-Int. Edit.*, vol. 44, no. 31, pp. 4844-4870, 2005.

24. Choi, S.; Park, S. H.; Ziganshina, A. Y.; Ko, Y. H.; Lee, J. W.; Kim, K., 'A stable cis-stilbene derivative encapsulated in cucurbit[7]uril,'*Chem. Commun.*, vol. 17, pp. 2176-2177, 2003.

25. Ong, W.; Gomez-Kaifer, M.; Kaifer, A. E., 'Cucurbit[7]uril: A Very Effective Host for Viologens and Their Cation Radicals,' *Org. Lett.*, vol. 4, no. 10, pp. 1791-1794, 2002.

26. Liu, S. M.; Ruspic, C.; Mukhopadhyay, P.; Chakrabarti, S.; Zavalij, P. Y.; Isaacs, L., 'The Cucurbit[n]uril Family: Prime Components for Self-Sorting Systems,' *J. Am. Chem. Soc.*, vol. 127, no. 45, pp. 15959-15967, 2005.

27. Wang, R.; Yuan, L.; Macartney, D. H., 'A green to blue fluorescence switch of protonated 2-aminoanthracene upon inclusion in cucurbit[7]uril,' *Chem. Commun.*, vol. 47,pp. 5867-5869, 2005.

28. Wang, R.; Yuan, L.; Macartney, D. H., 'Cucurbit[7]uril Mediates the Stereoselective [4+4] Photodimerization of 2-Aminopyridine Hydrochloride in Aqueous Solution,' *J. Org. Chem.*, vol. 71, no. 3, pp. 1237-1239, 2006.

29. **(a)** Freitag, M.; Gundlach, L.; Piotrowiak, P.; Galoppini, E., 'Fluorescence Enhancement of Di-*p*-tolyl Viologen by Complexation in Cucurbit[7]uril,' *J. Am. Chem. Soc.*, vol. 134, no. 7, pp. 3358-3366, 2012.

(b) Ivanov, D. A.; Petrov, N. K.; Nikitina, E. A.; Basilevsky, M. V.; Vedernikov, A. I.; Gromov, S. P.; Alfimov, M. V., 'The 1:1 Host−Guest Complexation between Cucurbit[7]uril and Styryl Dye**,**' *J. Phys. Chem. A*, vol. 115, no. 17, pp. 4505-4510, 2011.

(c) Kalmar, J.; Ellis, S. B.; Ashby, M. T.; Halterman, R. L., 'Kinetics of Formation of the Host–Guest Complex of a Viologen with Cucurbit[7]uril**,'** *Org. Lett.*, vol. 14, no. 13, pp. 3248-3251, 2012.

(d) Yuan, L.; Wang, R. B.; Macartney, D. H., 'Binding Modes of Cucurbit[6]uril and Cucurbit[7]uril with a Tetracationic Bis(viologen) Guest,' *J. Org. Chem.*, vol. 72, no. 12, pp. 4539-4542, 2007.

30. **(a)** Ramalingam, V.; Urbach, A. R.,'Cucurbit[8]uril Rotaxanes,' *Org. Lett.*, vol. 13, no. 18, pp. 4898-4901, 2011.

(b) Sinha, M. K.; Reany, O.; Parvari, G.; Karmakar, A.; Keinan, E., 'Switchable Cucurbituril–Bipyridine Beacons,' *Chem.-Eur. J.*, vol. 16, no. 30, pp. 9056-9067, 2010.

(c) Ke, C. F.; Hou, S.; Zhang, H. Y.; Liu, Y.; Yang, K.; Feng, X. Z.,' Controllable DNA condensation through cucurbit[6]uril in 2D pseudopolyrotaxanes,' *Chem. Commun.*, vol. 32, pp. 3374-3376, 2007.

(d) Kolman, V.; Khan, M. S. A.; Babinsky, M.; Marek, R.; Sindelar, V., 'Supramolecular Shuttle Based on Inclusion Complex between Cucurbit[6]uril and Bispyridinium Ethylene,' *Org. Lett.*, vol. 13, no. 23, pp. 6148-6151, 2011.

(e) Zhang, H. Y.; Wang, Q. C.; Liu, M. H.; Ma, X.; Tian, H.,' Switchable V-Type [2]Pseudorotaxanes,' *Org. Lett.* ., vol. 11, no. 15, pp. 3234-3237, 2009.

(f) Gao, C,; Silvi, S.; Ma, X.; Tian, H.; Credi,A.; Venturi, M.,'Chiral Supramolecular Switches Based on (R)-Binaphthalene–Bipyridinium Guests and Cucurbituril Hosts,' *Chem. Eur. J.*, vol. 18, no. 52, pp. 16911-16921, 2012.

31. Lee J. W.; Kim K.; Kim K., 'A kinetically controlled molecular switch based on bistable [2]rotaxane,' *Chem. Commun.*, vol. 11, pp. 1042-1043, 2001.

32. Anzenbacher P; Rodgers M. A. J., *Encylopedia of Supramolecular Chemistry*, Dekker, New York, 2004.

33. Silva A. P. ; Gunaratne H. Q. N.; Gunnlaugsson T.; Huxley A. J. M.; McCoy C. P.; Rademacher J. T.; Rice T. E., 'Signaling recognition events with fluorescent sensors and switches,' *Chemical Reviews*, vol.97, no.5 , pp.1515-1596, 1997.

34. Jun S. I.; Lee J. W.; Sakamoto S.; Yamaguchi K.; Kim K., ' Rotaxane based molecular switch with fluorescence signaling,' *Tetrahedron Letters*, vol.41, no.4, pp.471-475, 2000.

35. **(a)** Silva A. P.; Gunaratne H. Q. N.; Gunnlaugsson T.; McCoy C. P.; Maxwell P. R. S.; Rademacher J. T.; Rice T. E., 'Photoionic devices with receptor-functionalized fluorophores,' *Pure Appl. Chem.*, vol. 68, no. 7, pp. 1443-1448, 1996.

(b) Silva A. P.; Gunnlaugsson T.; Rice T. E., 'Recent evolution of luminescent photoinduced electron transfer sensors,' *Analyst*, vol. 121, no. 12, pp. 1759-1762, 1996.

36. Valuer,B.; Leary, I., 'Design principles of fluorescent molecular sensors for cation recognition,' *Coor.Chem. Rev.*, vol. 205, no. 1, pp. 3-40, 2000.

37. Valeur B., *Molecular Fluoresence,* Ed.; Wiley-VCH: Weinheim, Germany, 2002.

38. Turfan, B.; Akkaya, E.U., 'Modulation of Boradiazaindacene Emission by Cation-Mediated Oxidative PET,' *Org. Lett.* vol. 4, no. 17, pp. 2857-2859, 2002.

39. **(a)** Valeur, B.; Bourson, J. and Pouget, J., In: A.W. Czarnik, Editor, *FluorescentChemosensors for Ion and Molecule Recognition, ACS Symposium Series 538*, American Chemical Society, Washington, p. 25, 1993.

(b) Valeur, B.; Badaoui, F.; Bardez, E.; Bourson, J.; Boutin, P.; Chatelain A.; Devol I.; Larrey B.; Lefèvre J.P.; Soulet A.; *Chemosensors of Ion and Molecule Recognition, NATO ASI Series*, Kluwer, Dordrecht, p. 195, 1997.

40. Volterra V., 'Fluctuations in the Abundance of a Species Considered Mathematically,' *Nature*, vol. 118, pp. 558-560, 1926.

41. W. C. Bray, 'A Periodic Reaction in Homogeneous Solution and Its Relation to Catalysis,' *J. Am. Chem. Soc.*, vol. 43, no. 6, pp. 1262-1267, 1921.

42. Epstein I. R.; Showalter K., 'Nonlinear Chemical Dynamics: Oscillations, Patterns, and Chaos,' *J. Phys. Chem.* vol. 100, no. 31, pp. 13132-13147, 1996.

43. Briggs T. S.; Rauscher W. C., 'An oscillating iodine clock,' *J. Chem. Educ.*, vol. 50, no. 7, pp. 496, 1973.

44. Epstein R. I.; Polman J. A., 'An Introduction to Nonlinear Chemical Dynamics:Oscillations,Waves,Patterns, and Chaos,' *Oxford University Press*, 1998.

45. **(a)** Degn, H., 'Oscillating chemical reactions in homogeneous phase,' *J. Chem. Ed.*, vol. 49, no. 5, pp. 302, 1972.

(b) Noyes, R. M., 'Some models of chemical oscillators,' *J. Chem. Ed.*, vol. 66, no. 3, pp. 190, 1989.

(c) Nicolis G.; Portnow, 'Chemical oscillations,' *J. Chem Rev.*, vol. 73, no. 4, pp. 365-384, 1973.

46. Zaikin A. N.; Zhabotinsky A. M., 'Concentration Wave Propagation in Two-dimensional Liquid-phase Self-oscillating System,' *Nature(London)*, vol. 225, pp. 535-537, 1970.

47. **(a)** Rinker, R. G.; Lynn, S.; Mason, D. M.;Corcoran, W. H., 'Kinetics and Mechanism of Thermal Decomposition of Sodium Dithionite in Aqueous Solution,' *Ind. Eng. Chem. Fundamen.*, vol. 4, no. 3, pp. 282-288, 1965.

(b) Matzusaki, I.; Woodson J. H.; Liebhafsky, H. A., 'pH and Temperature Pulses during the Periodic Decomposition of Hydrogen Peroxide,' *Bulletin of the Chemical Society of Japan*, vol. 43, no. 10, pp. 3317, 1970.

48. Rabai, G.; Beck, M. T., 'High-amplitude hydrogen ion concentration oscillation in the iodate-thiosulfate-sulfite system under closed conditions,' *J. Phys. Chem.*, vol. 92, no. 17, pp. 4831-4835, 1988.

49. **(a)** Loudet, A.; Burgess, K.,' BODIPY Dyes and Their Derivatives: Syntheses and Spectroscopic Properties,' *Chem. Rev.* vol. 107, no. 11, pp. 4891-4932, 2007.

(b) Ziessel, R.; Ulrich, G.; Harriman, 'The chemistry of Bodipy: A new El Dorado for fluorescence tools,' A. *New J. Chem.* vol. 31, no. 4, pp. 496-501, 2007.

(c) Bozdemir, O. A.; Yilmaz, M. D.; Buyukcakir, O.; Siemiarczuk, A.; Tutas, M.; Akkaya, E. U.,'Convergent synthesis and light harvesting properties of dendritic boradiazaindacene (BODIPY) appended perylenediimide dyes,' *New J. Chem.* vol. 34, no. 1, pp. 151-155, 2010.

(d) Buyukcakir, O.; Bozdemir, O. A.; Kolemen, S.; Erbas, S.; Akkaya, E. U., 'Tetrastyryl-Bodipy Dyes: Convenient Synthesis and Characterization of Elusive Near IR Fluorophores,' *Org. Lett.* vol. 11, no. 20, pp. 4644-4647, 2009.

(e) Kim, H. J.; Kim, S. H.; Kim, J. H.; Lee, E. H.; Kim, K. W.; Kim, J. S., 'BODIPY Appended Crown Ethers: Selective Fluorescence Changes for Hg^{2+} Binding,' *Bull. Korean Chem. Soc.* vol. 29, no. 9, pp. 1831-1834, 2008.

(f) Coskun A., Akkaya E. U. A., 'Ion Sensing Coupled to Resonance Energy Transfer: A Highly Selective and Sensitive Ratiometric Fluorescent Chemosensor for Ag(I) by a Modular Approach,' *J. Am. Chem. Soc.*, vol. 127, no. 30, pp. 10464-10465, 2005.

(g) Coskun A., Akkaya E. U. A., 'Signal Ratio Amplification via Modulation of Resonance Energy Transfer: Proof of Principle in an Emission Ratiometric Hg(II) Sensor,' *J. Am. Chem. Soc.,* vol. 128, no. 45, pp. 14474-14475, 2006.

(h) Coskun A., Yilmaz M. D., Akkaya E. U. A., 'Bis(2-pyridyl)-Substituted Boratriazaindacene as an NIR-Emitting Chemosensor for Hg(II),' *Org. Lett.,* vol.9, no. 4, pp. 607-609, 2007.

50. Sindelar V., Silvi S., Kaifer E. A., 'Switching a molecular shuttle on and off: simple, pH-controlled pseudorotaxanes based on cucurbit[7]uril,' *Chem Commun.*, vol.20, pp. 2185-2187, 2006.

APPENDIX A

DATA

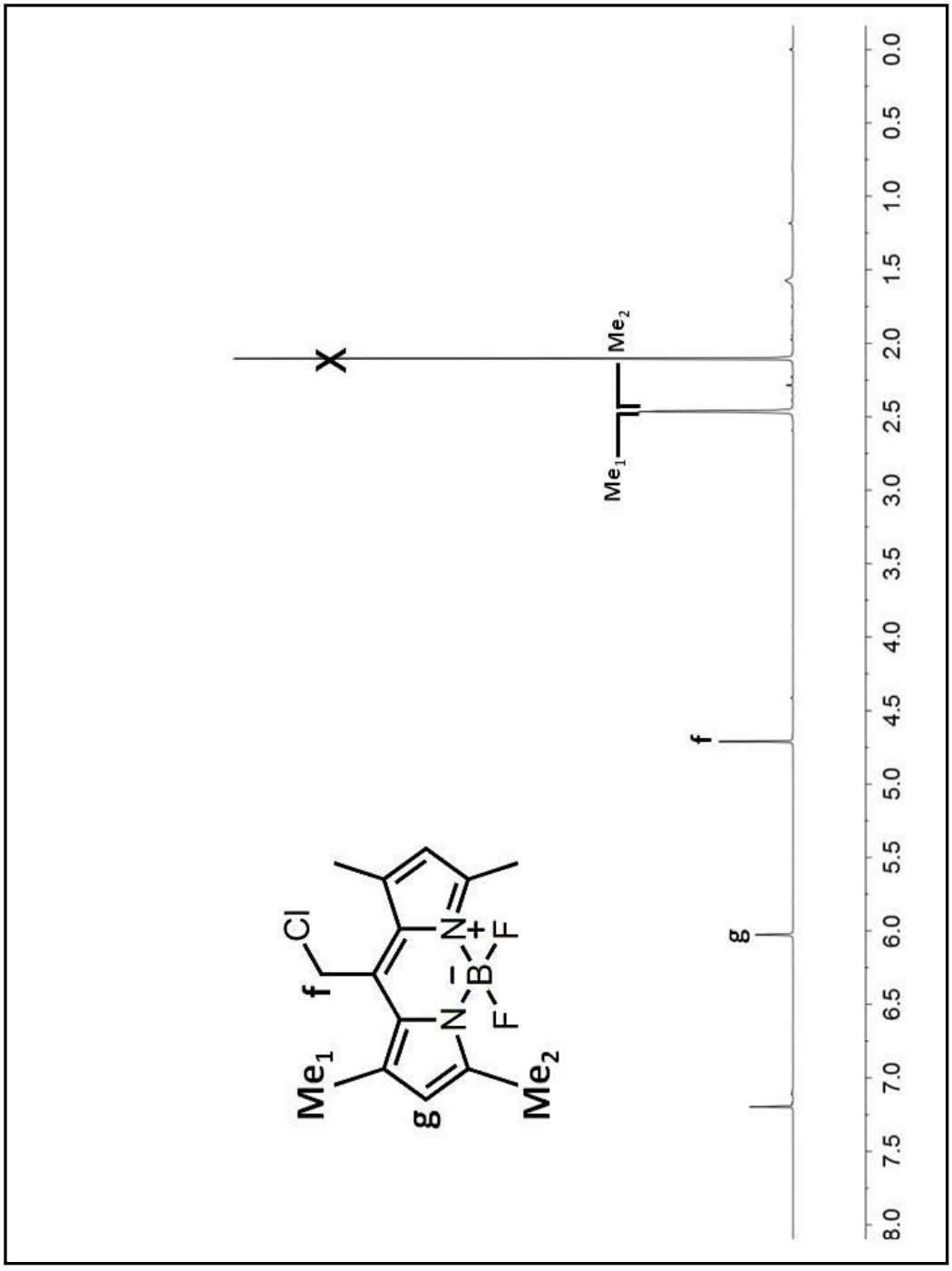

Figure 53. ^{1}H NMR spectrum of compound **1** recorded at 298K in $CDCl_3$.

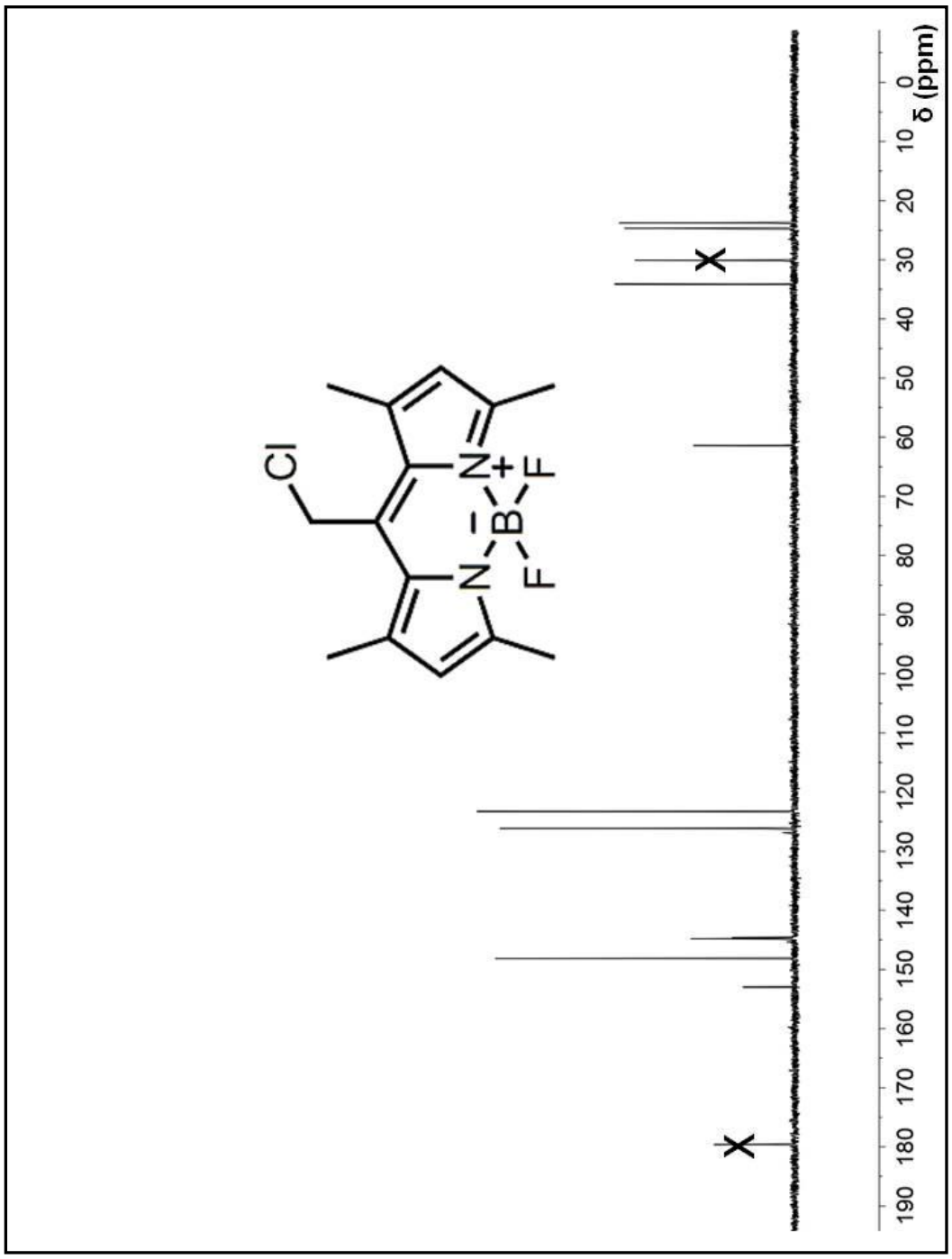

Figure 54. ^{13}C NMR spectrum of compound **1** recorded at 298K in $CDCl_3$.

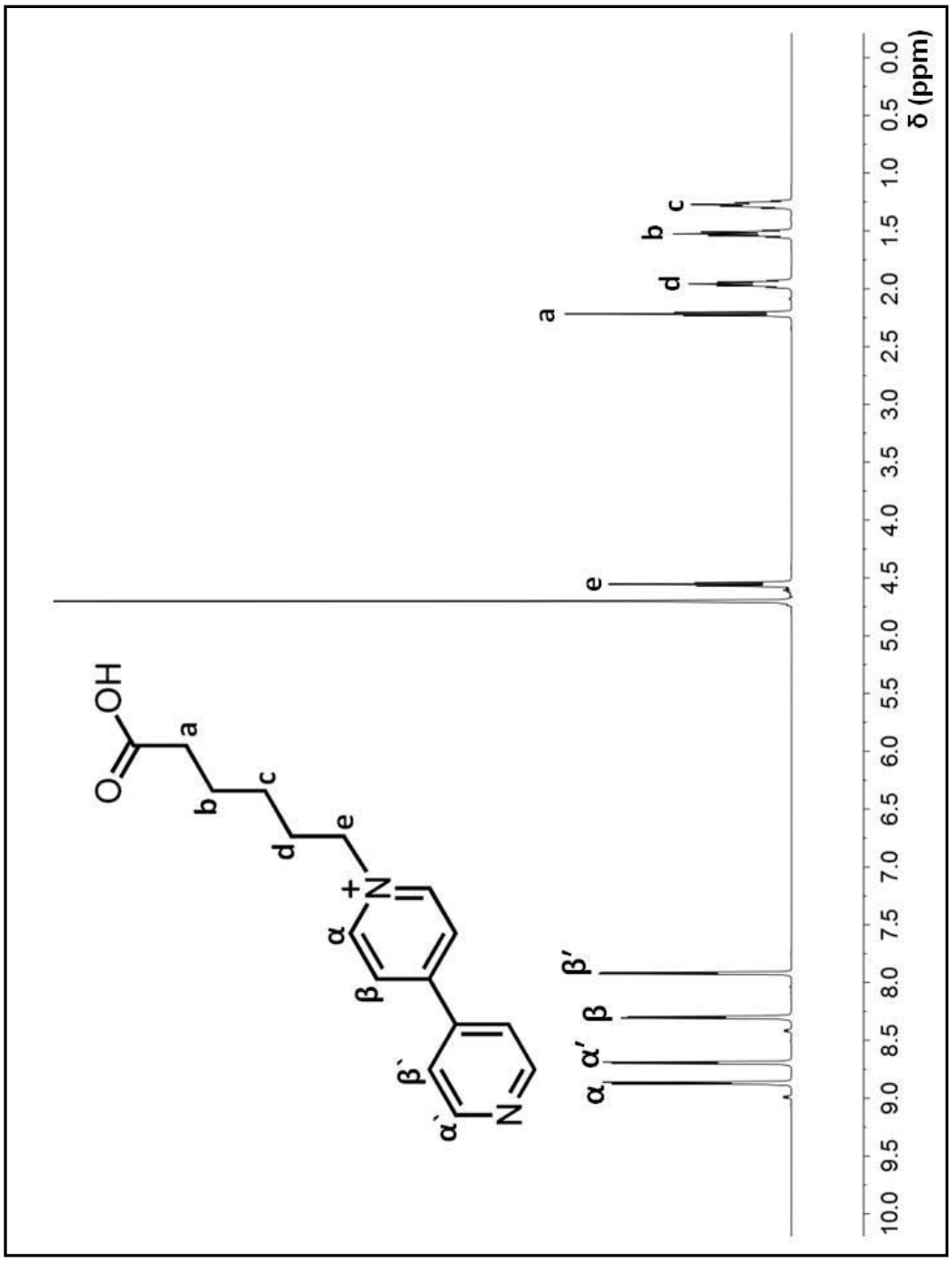

Figure 55. ^{1}H NMR spectrum of compound **2** recorded at 298K in D_2O.

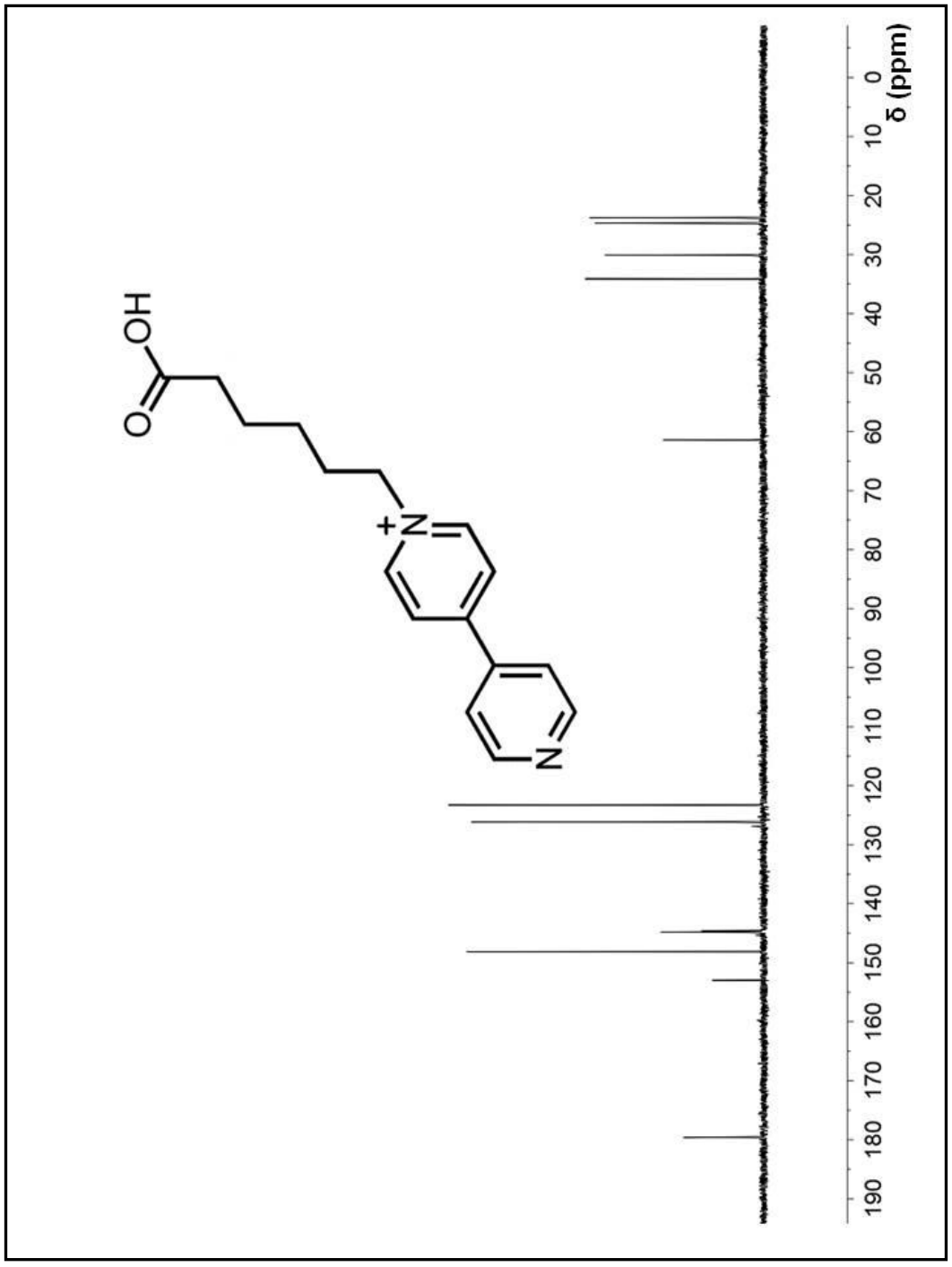

Figure 56. ^{13}C NMR spectrum of compound **2** recorded at 298K in D_2O.

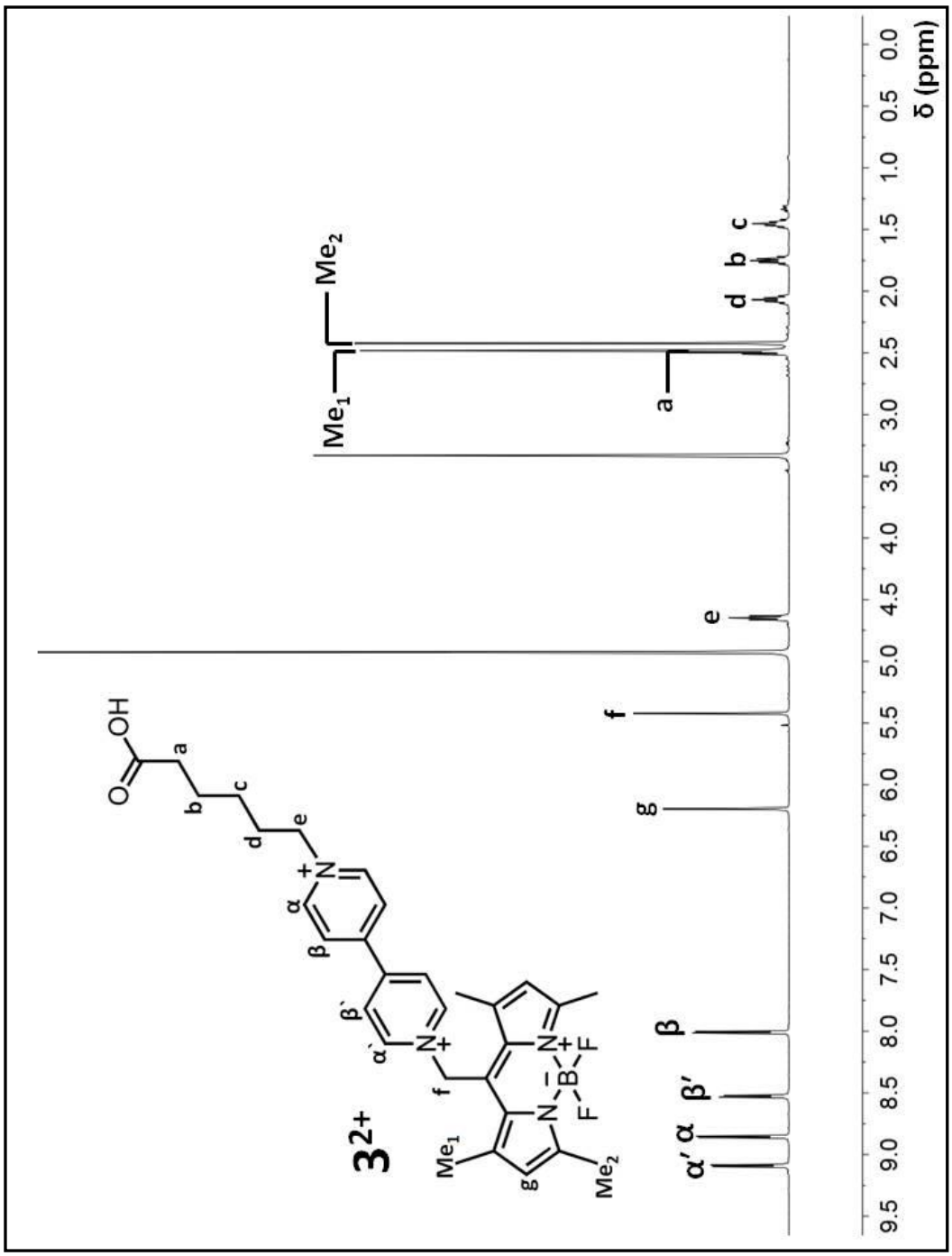

Figure 57. ^{1}H NMR spectrum of compound $\mathbf{3}^{2+}$recorded at 298K in CD_3OD.

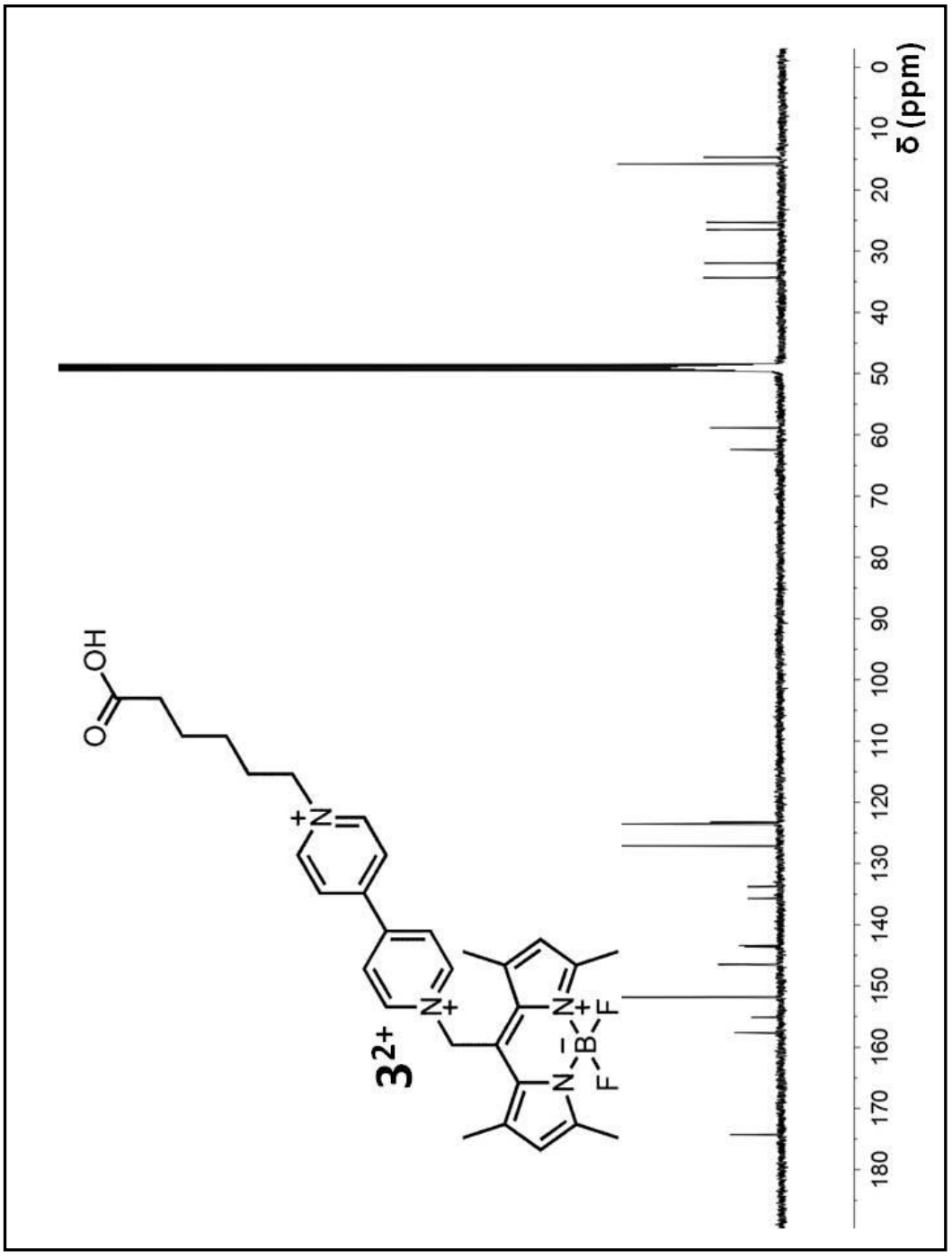

Figure 58. ^{13}C NMR spectrum of compound $\mathbf{3}^{2+}$ recorded at 298K in CD_3OD.

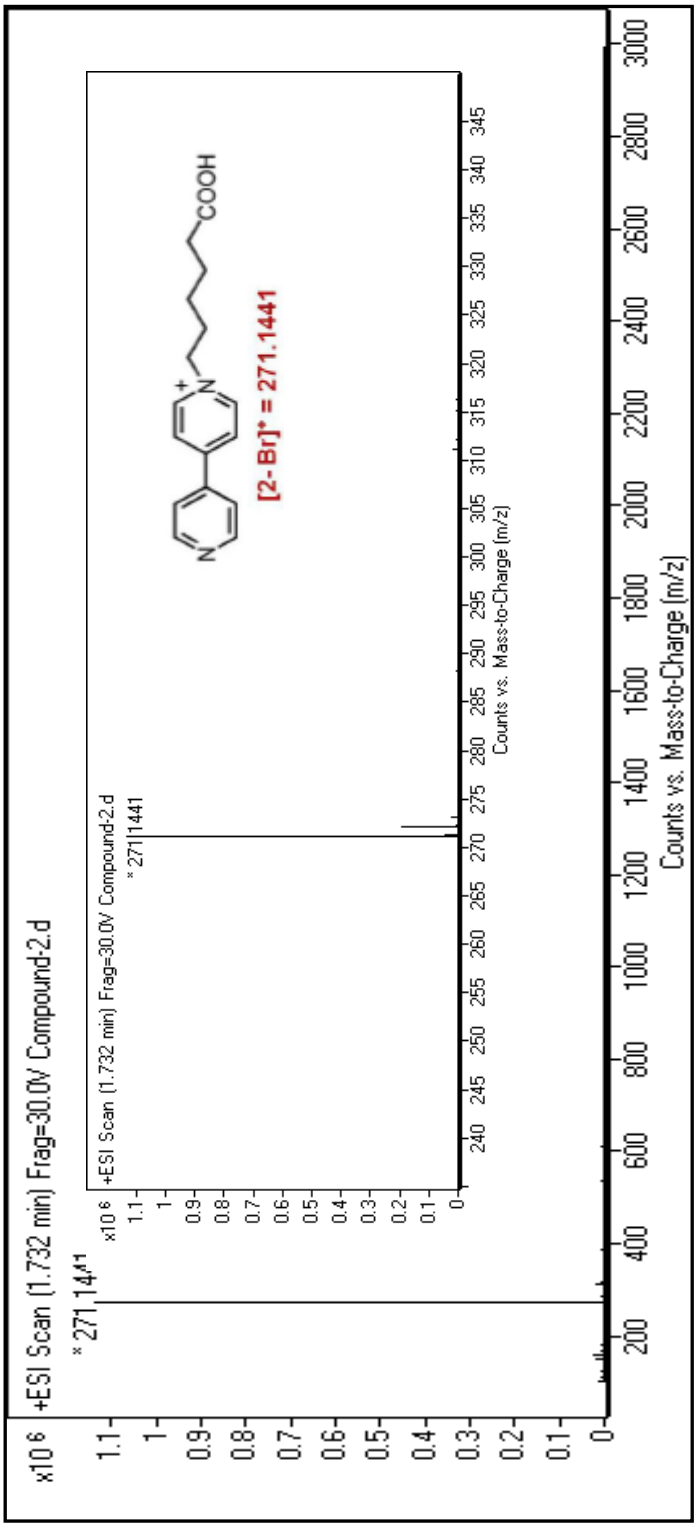

Figure 59. MASS spectrum of compound **2**.

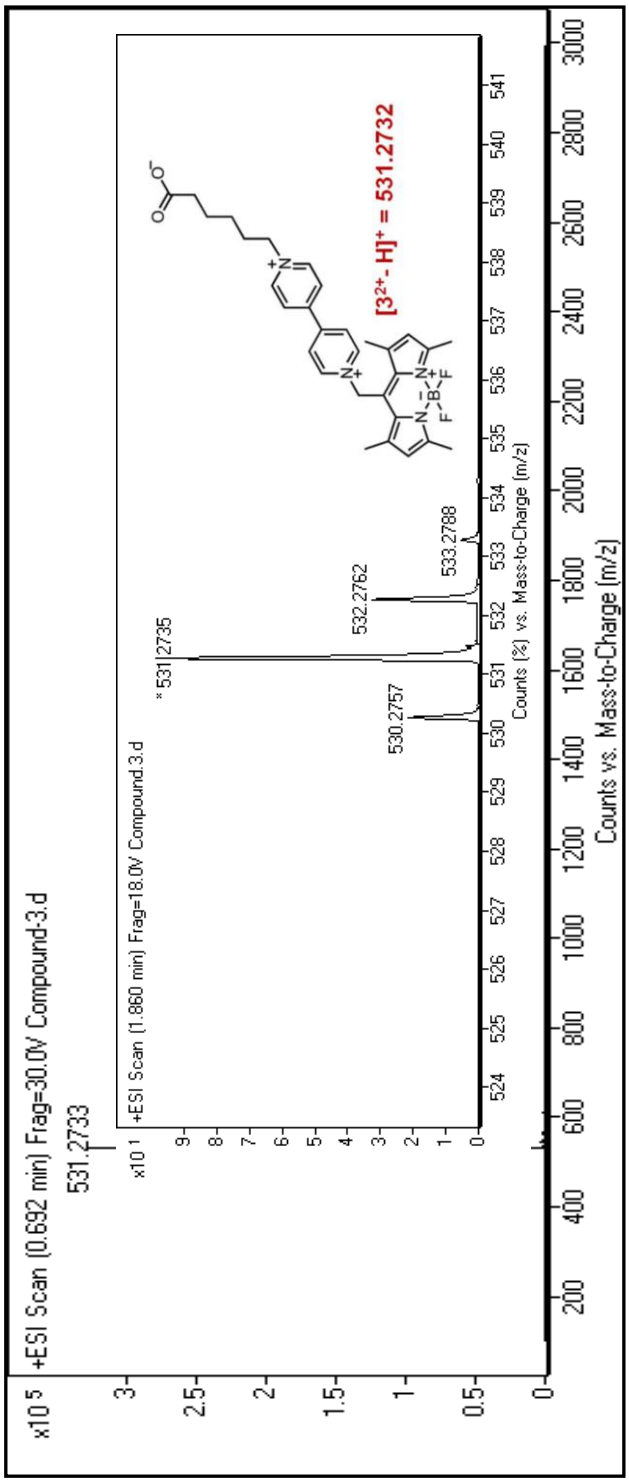

Figure 60. MASS spectrum of compound $\mathbf{3}^{2+}$.